University of Stavanger

FACULTY OF SCIENCE AND TECHNOLOGY

BACHELOR'S THESIS

Study programme/specialisation: Petroleum technology	Spring semester, 2021 Open / ~~Confidential~~
Author: Erik Bukkholm	
Programme coordinator: Supervisor(s): Pål Østebø Andersen Reidar I. Korsnes	
Title of bachelor's thesis: **Reactive flow in chalk at reservoir temperature – Experiment and simulation**	
Credits: 20	
Keywords: Chalk Reaction Kinetics Chemical Analysis Simulation	Number of pages: 52 + supplemental material/other: 0 Stavanger, 15.05.21 date/year

Contents

Abstract

This thesis seeks to study how 0.219 M $MgCl_2$ brine flooded through chalk cores at reservoir temperatures will chemically react when flooded through at various flowrates. We used two different chalk cores. The cores were from Stevns Klint in Aalborg, Denmark and Kansas, USA and are referred to as SKA3 and KR30 respectively. A triaxial cell was used for each of the cores for this experiment, with SKA3 being run at 100ºC and KR30 at 130ºC. Pore pressure and confining pressure was maintained at a constant level throughout the experiment, only the flowrate was varied. For SKA3 a pore pressure 0.7 MPa and a confining pressure of 2.0 MPa was used, while KR30 was run at equal pore pressure but lower confining pressure (1.2 MPa). The confining pressures were deliberately low in order to minimize compaction of the cores. The effluents were sampled regularly and then analyzed with an ion chromatography machine to see how varying the flowrate affects the concentrations of ions present in the brine after flooding. From plotting these results, we could see a general trend that lowering the flowrate increased the concentration of calcium present in the effluents. This shows that the brine had a greater chemical effect on the chalk when the flowrate was lower. At higher flowrates, the opposite behavior was shown. The data gathered from core SKA3 showed a greater tendency to deviate from this behavior, often failing to reach steady state. Core KR30 showed no deviation from the general trend, with lower flowrates always increasing calcium concentration and vice versa. Comparing these results with similar tests performed on Stevns Klint cores from the same block as SKA3 (Olsen, A. T, 2020) suggest that temperature was the deciding factor in the trouble to reach steady state, not the chalk type. After completing the floodings the gathered data was then compared to a model developed to predict the concentrations of ions in the flooding of a chalk sample by $MgCl_2$-based brines. A set of mathematical equations was solved to predict ion concentrations at different rates. The tuned model was plotted alongside the experimental measurements for comparison. We were able to fit the model to a satisfactory degree, where it was able to reasonably predict the concentrations of the ions at a given flowrate.

Acknowledgements

I would like to thank my supervisors Dr. Korsnes and Dr. Andersen for their patient and efficient guidance for the duration of the thesis. Their knowledge and experience have been invaluable in terms of writing this thesis and I have learned incredibly much over the course of this semester.

1   Introduction

Chalk formations are formed by large amounts of dead sub-microscopic plankton which then settles on the bottom of oceans. The plentiful nature of these creatures means that we will frequently encounter chalk formations when drilling for hydrocarbons.
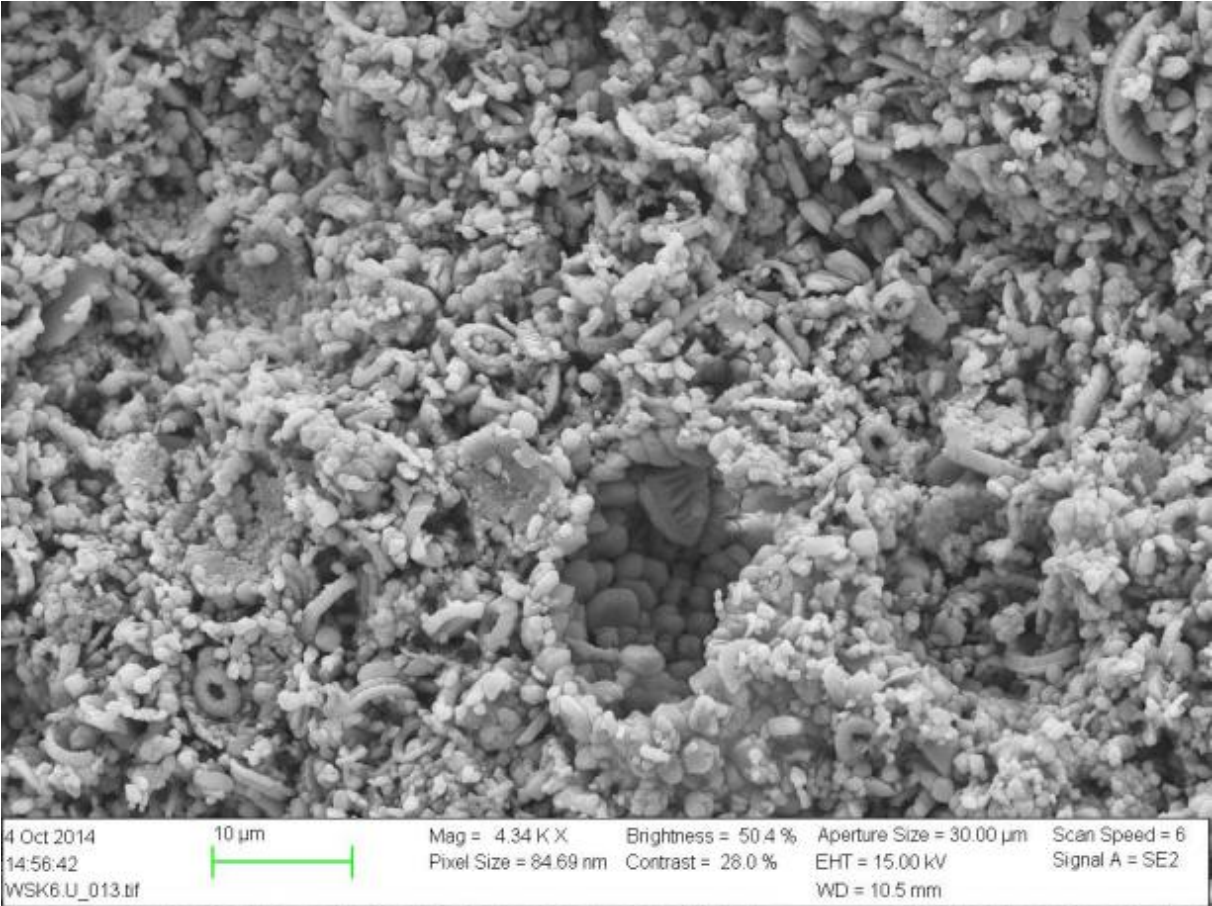
Figure 1: Chalk at microscale (Minde, 2014)

Chalk will react with water upon contact, and this can present challenges when drilling through chalk formations. The reaction between chalk formations and seawater leads to a measurable dissolution of the chalk and can cause the formation to compact as a result, through an effect known as water-weakening (Madland et al, 2010). As compaction can cause for example subsidence of the ground above the reservoir, this can cause a great deal of trouble for continued drilling operations. An option is to switch to an oil-based mud, but water-based muds are generally preferred as they are cheaper and easier to produce (by using readily available sea water). In these water-based muds inhibitors are often used to limit its reactivity with the

environment.

That water will react with chalk and cause erosion to the chalk is well known, but at reservoir conditions we have many variables in pressure and temperature which can affect exactly how quickly these reactions play out. Knowing the behavior of chalk in these different scenarios could be helpful for a drilling crew, allowing them to make better operational plans and avoid danger.

Despite the great differences between different oilwells and reservoir they all share one common trait. They are reliant on the internal pressures of the reservoir to get the oil from the reservoir to the surface. As more and more oil is removed from the reservoir this pressure will naturally begin to drop, and less oil can be produced. In order to extract as much oil as possible the reservoir will therefore need to be artificially altered to regain the pressure and keep producing oil. This process is known as secondary oil recovery and is carried out by using either water or gas injection to maintain pore pressure or displace the petroleum towards the oilwell. As secondary oil recovery requires the manipulation of natural formations, great care is taken to ensure that the environment is not adversely affected. In our case we are looking at the effect of using a $MgCl_2$-based brine as the injected fluid. This will affect the structural integrity of the formation through the dissolution of calcite. (Madland et al, 2011) This is relevant for this thesis because we wish to study how the rate of injection and temperature of the formation affects the interaction between the brine and the calcite. In practice the brine injected into for example North Sea chalk formations will never be a "pure" magnesium-brine but will rather be a brine containing many different salts and components. The reason for why we are studying magnesium in particular is because previous research has shown that this ion is especially important in terms of enhanced oil recovery and water weakening (Austad et al, 2007). How different types of chalk affects the reactions is also of interest.

The first discovered oil field on the Norwegian continental shelf was the Ekofisk field, and it is arguably still the most famous. Ekofisk is a chalk field, and at its discovery it had a reservoir it had a reservoir pressure of 7135 psia (~490 bar) at 10400 ft. The field also initially contained an undersaturated volatile oil with a bubble point pressure of 5560 psia (~383 bar) and a temperature of 268°F (~130°C). The oil being undersaturated means that it is currently at a higher pressure than the bubble point pressure, the pressure at which the oil will begin releasing dissolved gas contained within it. In practice this means that it contains less gas than it is

theoretically able to dissolve. As oil production begins the reservoir pressure will eventually drop below the bubble point pressure. The initial recovery factor as production began was estimated to be at 18% recovery using gas reinjection. Waterflooding was initially not considered as a viable option for increasing production, given that the chalk was assumed to be either intermediate-wet or at worst oil-wet. This meant that flooding with a water-based brine would be ineffective, for reasons which will be explained in a later section. Water injection tests had been conducted already in 1979 but was not done on a large scale for the purpose of enhanced oil recovery before 1987. Current estimates on total oil recovery from Ekofisk now sits at 50-55%, clearly indicating the success of water injection. This success, in addition to an earlier discovery (in 1984) that the seabed was subsiding because of reservoir compaction, led to an increased interest in researching exactly how injection of seawater and other solutions would affect a chalk reservoir (Hermansen et al, 2000).

Subsidence of the ground or of the seabed occurs as the formations beneath the surface starts to compact, in our case because of the production of hydrocarbons. As previously discussed, chalk reservoirs form as coccolithophorids accumulate on the seabed over a long period of time, gradually building up more and more layers of material. At the early stages of this process the layers of chalk are not heavy enough to consolidate it into rock, making the chalk behave more like a liquid with solid particles in suspension. Eventually, the mounting weight of successive upper layers will start compacting the lower layers. During this stage, the liquid contained in the lower levels tries to escape through fluid pathways. This reduces the amount of pore space in the chalk as it gets filled in when the liquid escapes. If the overlying strata become impermeable any remaining liquid will be unable to escape. The fluid pressure now starts to rise beyond the standard hydrostatic pressure and the fluid itself becomes integral in the stability of the structures in which it is now trapped. This fluid overpressure can also occur if the rate of sedimentation is to high compared to the expulsion rate. When liquid is produced from the reservoir the pore-fluid pressure is decreased but the weight of material above remains the same, compacting the formation and causing subsidence. At high levels of subsidence equipment such as the casing lining the well walls can become stretched or compacted to the point of failure, and the oilrig itself can be lowered to the point where waves might start hitting the lower decks.

Chalk consists mainly of calcium carbonate, $CaCO_3$, though some level of impurities is generally also present. In order to dissolve the chalk rock, as a method of reducing its strength,

one needs to use brines containing ions that will separate the calcium ion from the carbonate molecule. Studies have shown that at high temperature, brines containing Mg^{2+} and/or SO_4^{2+} effect on chalk rocks (Korsnes et al, 2007; Heggheim et al, 2005; Nermoen et al, 2016). The way sulfate specifically affects the mechanical strength is discussed in (Megawati et al, 2012). It found that the bulk modulus and yield point of a chalk sample is reduced significantly by flooding it with a Na_2SO_4 brine at elevated temperatures. This occurs because the sulfate negatively charges the calcite surface. The interaction between charged surfaces specifically in the weak overlaps of electrical double layer gives rise to the total disjoining pressure in granular contacts. The net repulsive forces act as normal forces in the grain's vicinity, counteracting the cohesive forces and enhance pore collapse failure during isotropic loading. Temperature was deemed to influence the adsorption of sulfate, with a sulfate adsorption of 0.3 µmol/m^2 at 50°C and 0.7-1.0 µmol/m^2 at 130°C. The magnesium also serves to weaken the rock matrix of the chalk, but it works in a different manner. When magnesium brine interacts with the chalk a substitution reaction between the calcium carbonate ($CaCO_3$) and the magnesium chloride ($MgCl_2$) occurs, which produces magnesite ($MgCO_3$). This process therefore primarily weakens the chalk material changing its mineralogy, as opposed to the sulfate which weakens the material by coating its surfaces in a substance that causes them to resist each other (Megawati et al, 2013). In this thesis we are looking mostly at magnesium interaction. A recent study on how floodings by the same brine under the same conditions will affect different chalks has also been put forward by Andersen, et al, 2018. Five different outcrop chalks where selected from five different locations. These locations were: Kansas, Mons, Liège, Aalborg & Stevns Klint, sorted from old to young. The cores were flooded for a period of 60-95 days, except for the Stevns Klint and Aalborg cores which were flooded for 45 and 115 days, respectively. The floodings were done using 0.219 M $MgCl_2$ brine at 130°C at a confining pressure ranging from 8.5 to 23 MPa, emulating typical reservoir conditions. As the level of purity (and thus the total amount of calcite) varied from core to core, the proportion of Mg-bearing minerals varied from sample to sample and could not be applied for all types of chalk. All chalks were however found to have precipitated Mg-bearing minerals. The study showed that chalk type can have an impact on the distribution of newly formed Mg-bearing minerals with varying peaks of enrichment. Cores with higher SiO_2 content showed more compaction when injected with $MgCl_2$ brine.

Of interest is also the phenomenon of spontaneous imbibition. This occurs when capillary forces draw liquid into constricted spaces without the assistance of external forces and is reliant on the

wettability of the spaces the liquid tries to enter. In terms of EOR, this effect is desirable for its ability to displace the oil in the spaces new liquid is drawn into. Wetting involves the interaction of a liquid with a solid. It can refer to the spreading of a liquid over a surface, the penetration of a liquid into a porous medium, or the displacement of a liquid by another liquid (Berg, 1993). Methods of modifying the wettability of reservoir rocks using various brines is therefore being researched heavily (Standnes & Austad, 2000; Puntervold et al, 2015). The point here is that oil can only be displaced from pores where the displacing liquid can reach. If the surface of the reservoir rock resists contact with the displacing liquid it will not be able to penetrate as deep into the reservoir rock and therefore displace far less oil. One of these studies (Austad et al, 2007) found that various surface active components present in seawater, among them Mg^{2+} and SO_4^{2-}, play an important role in modifying the wettability of the chalk. When Mg^{2+}- and SO_4^{2-} containing water was imbibed into the chalk rock the wettability was determined to have been changed. As mentioned, water injection at Ekofisk was originally only done in order to repressurize the formations and try to prevent further subsidence of the ground. It was discovered however that injecting the seawater had a big impact on the oil recovery, being the primary reason for why the expected recovery rate sits at over 50% today.

Research is also being conducted to see how flooding actual reservoirs with reactive brines will affect them. In a full-scale reservoir, the pumped in liquid will flow differently from how it flows through a chalk sample in a closed system. For example, porous chalk reservoirs typically contain large fractures. These fractures are typically far less resistant to flow than the pores, meaning that liquids prefer to be channeled down these fractures rather than force their way into the actual pores. Here spontaneous imbibition is important, as these forces help draw the brine into the pores that would otherwise escape down the fractures. Given that most carbonate reservoirs are fractured to a greater or lesser degree, the difference between a real-world flooding of a reservoir and the flooding of a core sample in a lab could be significant. (Austad et al 2005; Zhang et al, 2007).

In 2012 a geochemical model was developed which considers the combined effect of transport and chemical reactions in chalk and uses them to predict the ionic concentration for brines flooded through a chalk core in experimental settings (Andersen et al, 2012). This model builds upon the findings of (Evje et al., 2009; Madland et al., 2011), which produced the first version of a mathematical model. In 2019 a further development to the model was made by Andersen

& Berawala (2019). In 2020 the work was continued for the bachelor's thesis of Andre Tvedt Olsen. He carried out tests using two SK cores (called SK1 and SK2, drilled from the same block as SK3 used in this study) at the same temperature, but with two separate brines. These were both $MgCl_2$-based brines; one at a concentration of 0.219 moles, and the other at 0.0445 moles. These tests are still being run at the point of writing this thesis. We will be testing a SK core at 100°C to look at the effect of temperature and a Kansas core at 130°C to see if a different chalk type has notably different effluents from that of a another. We will be using a 0.219 M $MgCl_2$ brine in the flooding of both cores. From previous experiments we know that temperature has a profound impact on fluid effect (Madland et al, 2008). From the unpublished works of (Olsen A.T, 2020) we know that flowrate also affects it.

1.1   Objectives

The purpose of this thesis is to describe how the chemical reactions between a $MgCl_2$ brine and a chalk rock sample ($CaCO_3$) behaves at varying flowrates and temperatures, and to see if this behavior can be accurately modeled using the mathematical model developed by (Andersen & Berawala, 2019). We vary the flowrate in order to see how much this affects the concentration of magnesium and calcium ions in the sampled effluents, which will then allow us to tune the model in a way that tells us how the concentrations of ions will look at any given flowrate. The flowrates will be range from 0.25 to 8 PV/day based on earlier experiments. Temperatures have been selected based on temperatures typical for oil reservoirs, such as the temperature of Ekofisk which is at 130ºC. earlier experience If the validity of said model can be made to reliably represent the experimental behavior it can be used to more accurately describe the findings of future, similar experiments. If the model is proven to be inaccurate however, the data gathered in this thesis can potentially be used to make improvements to it. A similar experiment was carried out by Andre Tvedt Olsen in 2020 for his BSc thesis. This experiment will use different chalk types and temperatures to see how this might change the results.

1.2   Outline

Chapter 2 will contain two sections. The first of these sections will be theory concerning the chalk. Here the nature of chalk formation will be explained, as well as the chemical solubility of chalk.

Chapter 3 will present the experimental setup and techniques used such that the experiment can

be replicated by others.

In chapter 4 the results from the experiment will be presented and be compared and fitted to the model.

Chapter 5 will discuss the results of the experiments and possible sources of error.

2 Theory

2.1 Chalk

Chalk is a highly porous mineral composed of calcite ($CaCO_3$). In its pure state it is white and highly porous. It is classified as a sedimentary carbonate rock and is formed from the gradual accumulation of primarily calcite shells shed by microscopic coccolithophores. Other creatures, such as foraminifera may also contribute to this accumulation of matter. As the layers build up and pressure increases the loose mass eventually hardens into solid rock. Studying the resultant structures under a microscope will reveal that many of the skeletal structures remain intact, giving further evidence that the material makeup of this rock stems from these ancient creatures.

The individual particles of the chalk rock will generally range in size from 0.5 to 3 microns, with pore throats ranging from 0.1 to 1 micron. Despite the typically high porosity of chalks, they still exhibit low permeability. For example, chalks with porosity in the 35-45% range will in favorable conditions have a permeability of just 1-3 mD. (Hardman 1982)

Not all chalks are perfectly pure. In this experiment both a highly pure (>99% calcite by weight) Stevns Klint core and a more impure (~97%) Kansas core will be used. The impurities of the Kansas core are primarily clay (Andersen et al, 2018).

For a chalk formation to become a reservoir for hydrocarbons it first needs to become saturated with them. This means that the migrating hydrocarbons need to overcome the resistance of the formations low permeability to enter the pores of the system. As the hydrocarbons begin to accumulate underneath the chalk, pressure also starts to increase. As more and more hydrocarbons migrate into the constricted space, the pressure will get higher and higher. At a certain point, the pressure needed to overcome the resistance of the low permeability is surpassed and the hydrocarbons will simply force themselves into pores of the chalk. Chalks with large pore throats are better reservoirs than those with smaller pore throats, as the pressure

needed to saturate them are lower. (Hardman 1982)

2.2   Solubility

Solubility is the ability of a substance, in any state of matter, to dissolve in a solvent. The ability of the substance to dissolve depends on both the solubility of the substance you are trying to dissolve and the type of solvent you are using. NaCl for example has a solubility of 360 g/L in water, but only 14,9 g/L in ammonia. The solubility of a substance can be determined mathematically by using the following formula:

$$K_{sp} = [C]^c[D]^d \quad (1)$$

Here K_{sp} is the solubility product constant, and C and D is the concentration of ions C and D which the substance has been dissolved to. K_{sp} gives an indication of how much. as an example, for calcium carbonate dissolved in water the formulas might look something like this:

$$CaCO_3(s) \leftrightarrows Ca^{2+}(aq) + CO_3^{2-}(aq) \quad (2)$$
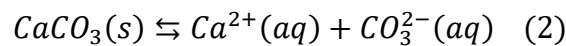
giving K_{sp} as

$$K_{sp} = [Ca^{2+}] * [CO_3^{2-}] \quad (3)$$

In this thesis we are particularly interested in the solubility of minerals in water as we will exclusively be using a water based $MgCl_2$ solution. We expect the substitution reaction between the calcium and magnesium to be the primary driver behind the chalk dissolution, but the effect of general dissolution from the water itself is also contributing factor.

The solubility of minerals in water varies greatly. Some are easily dissolved in room temperature and remain suspended in solution afterwards, while others might be insoluble in the same conditions. The solubility of a substance can be increased however. Rather unusually calcium carbonate becomes more soluble in lower temperature water (Appelo & Postma, 2004). When a substance dissolves in water its outermost cations will be drawn towards the negative side of the water molecule, and the anions will be drawn to the positive side. These water molecules will then surround the now dislodged ion, suspending it in the water (Appelo & Postma, 2004).

The dissolved substance will then reach equilibrium. Equilibrium is a state were no more substance can be dissolved. This phenomenon is described as follows by Guldberg-Waages law:

$$aA + bB \leftrightharpoons cC + dD \quad (4)$$
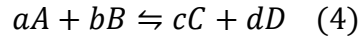
The upper-case letters refer to the substance in question and the lower-case letters refer to the number of moles of each substance. The arrows in the middle pointing in opposite direction shows that the reaction happens both ways. Which way the reaction "prefers" to happen can be described by the equilibrium constant K:

$$K_C = \frac{[C]^c [D]^d}{[A]^a [B]^b} \quad (5)$$

Here A and B are the concentrations of each reactant, while C and D are the concentration of each product. K is given as K_C because it is expressed in terms of concentration. If K is large, it means that the concentration of products is high, meaning that the equilibrium is skewed towards the right. Low values of K naturally mean the opposite is true.

2.2.1 Effective concentration

Typically, in real world scenarios a solution will react to a lesser degree than the concentration of ions it contains would suggest. This is because minute variations in energy levels among the ions in the solution will prevent some of them from reacting, thus limiting the total amount of reactions which can take place. This means that the solution is going to have what is known as an "effective concentration" of the ions suspended in it, in the sense that solutions chemical potential depends on the activity of a real solution in the same way that it would depend on the concentration in an *ideal* solution. This phenomenon is dependent on molality and the ionic strength (Appelo & Postma, 2004). Molality means the number of moles of solute present in one kg of solvent.

3   Experiment

The experiments consisted of $MgCl_2$ brine floodings at different constant flowrates. Throughout the tests only the flowrate will change, the confining pressure and temperature will be unaltered. During the flooding itself pore pressure will be kept constant. The cores will be flooded in two

separate triaxial cells until the reactions are assumed to be at steady state, at which point the flowrate will be changed. Whether steady state has been reached or not will be determined based on the measured concentrations of ions in the effluents. If several consecutive samples show equal or near equal results, we will assume steady state has been reached. The flooding will then continue until steady state has been achieved again. This process will be repeated several times, both by lowering and increasing the flowrate.

3.1 Test setup

The experimental setup can be divided into the following parts:

- The preparation of the core samples.
- The preparation of the brine.
- The preparation of the triaxial cell.
- The flooding and effluent collection

3.1.1 The core samples

Two different core samples were needed for this experiment, one Stevns Klint (SK) sample and one Kansas (K) sample. The cores had been cut before the experiments were started but contained moisture. This was removed in a heating chamber at 100ºC. Both the dry cores were weighed. To ensure consistent and comparable results the same cores were used for the full duration of the experiments. The properties of these cores are given in table 1.

Table 1: Core properties

Chalk Sample	L (mm)	D (mm)	Dry weight (g)	Wet weight (g)	Porosity (%)
SKA3	71.25	38.03	119.45	156.22	45.43
KR30	74.46	38.05	141.23	173.79	38.46

3.1.2 Saturation

When all moisture in the cores had been eliminated, they were saturated with distilled water.

This was done with a small vacuum chamber. The core was placed in a small cup and put into the chamber before a vacuum was drawn. Once the pressure in the chamber was low enough distilled water was dripped into the cup until the core was completely submerged. The chamber was agitated slightly to ensure that the core was properly saturated. The vacuum chamber with the core placed inside is shown in figure 1. After this the cores were weighed to determine the saturated mass.

Figure 1: Core saturated with distilled water by using vacuum.

3.1.3 Porosity

The samples were weighed in both the dry and saturated state in order to accurately calculate their porosity. This was done using the following formula:

$$\Phi = \frac{V_p}{V_b} = \frac{\dfrac{W_{sat} - W_{dry}}{\rho_f}}{\dfrac{D^2}{4} \times \pi \times L}$$

- Φ = Porosity
- V_p = Pore volume
- V_b = Bulk volume
- W_{sat} = Weight of water saturated core
- W_{dry} = Weight of dry core
- D = Core diameter
- V_p = Bulk volume
- L = Core length
- ρ_f = Fluid Density

3.1.4 Brine

The brine used in the experiments was a 0.219 M $MgCl_2$ solution. It was made by first mixing distilled water to with calcite powder until equilibrium. Before use the solution was filtrated through a 0.22 µm MCE membrane of the type MF-Millipore. After this, 44.5 g of $MgCl_2 \times 6H_2O$ was added into one liter of this calcite solution. The $MgCl_2$ was then stirred into the solution until fully dissolved. The solution was filtered through a 0.65 µm MCE membrane of type MF-Millipore to remove any potentially remaining solids. A vacuum pump was used to pull the solution through the membrane.

3.1.5 Placing the core in the triaxial cell

The core for each cell was prepared by first placing a gasket and a distribution disk on either end with a filter paper between the distribution disk and core, Fig 2a and b. They were then fully enclosed with a heat shrinking plastic sleave, Fig 3a. The gaskets and the plastic sleave ensured that the cores remained completely sealed off from the rest of the system, and the distribution disks ensured that the brine would evenly permeate the core. An extensimeter was then installed around the core to measure the diameter of the core. The assembly's top piston was fitted with a steel tubing that was connected to the bottom part to let the water back out of the cells. This part of the assembly process is shown in figure 3b. The cell is known as a triaxial cell and contains both a top and bottom piston.
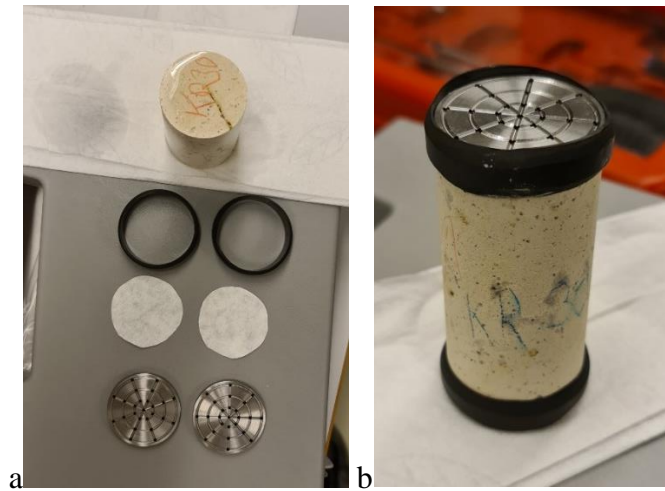
Figure 2: (a) Core assembly parts (Distribution discs, filter papers and rubber gaskets from bottom to top) (b) All assembly parts fitted to core
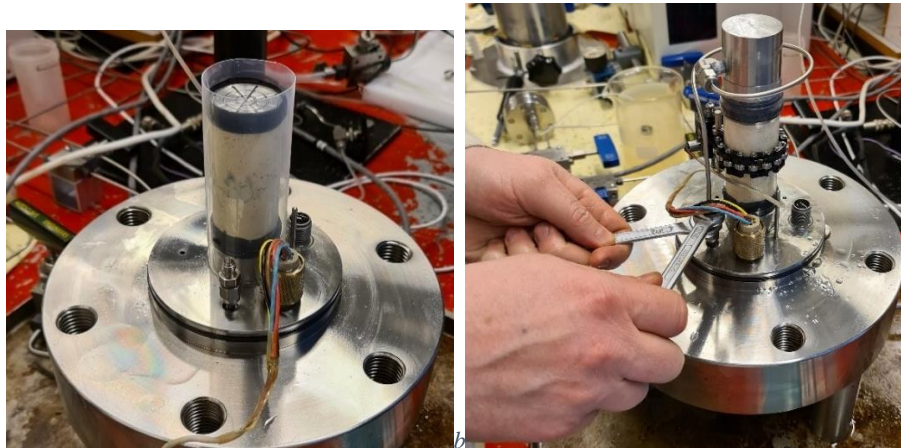

Figure 3 (a) Core assembly placed in cell and (b) outlet tubing and extensimeter being attached.

3.1.6 Completing the cell

When the core sample had been placed on the cell, a steel cylinder was placed around it. A heating jacket was then fitted to the outside of the cylinder. The space between the core assembly and the cylinder was then filled with marcol 82. This oil is pressurized to give the desired confining pressure. The fitted steel cylinder and heating jacket is shown in the left image of figure 4a. The added marcol 82 is visible in said image. The head of the cell was then placed on top and fastened by six large bolts. A torque driver was used to fasten them to 150 Nm of torque, Fig 4b. Finally, a linear variable differential transformer (LVDT) was placed on the cell

head, Fig 5. This would allow us to measure the length of the core during the experiment.

The cell itself is made of thick steel to withstand the pressures which the experiment demands. The confining pressure for this experiment will not exceed 2.0 MPa in either cell, which the cells will be able to withstand without much concern. The pressure was measured by gauges connected to the cell.
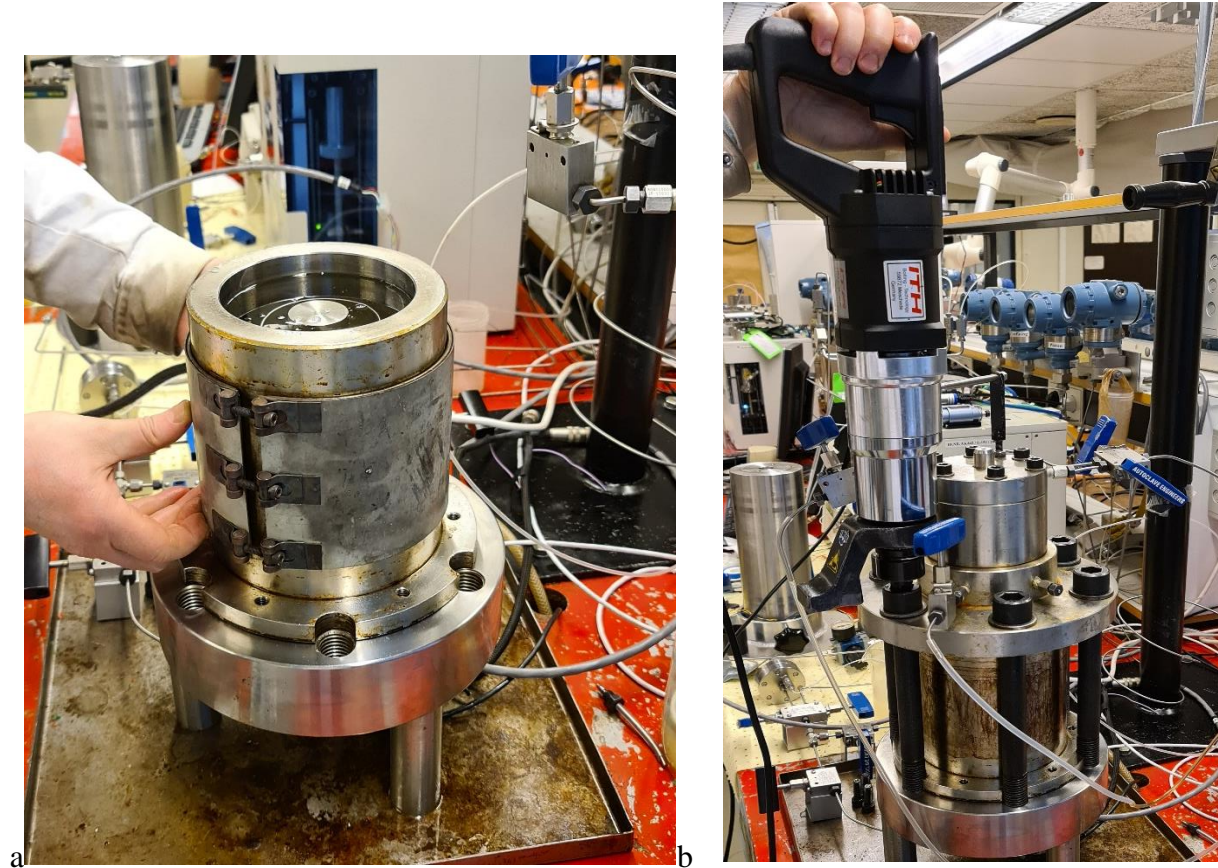

a b

Figure 4: (a) Steel cylinder and heating jacket fitted, and (b) cell head attached with torque driver.
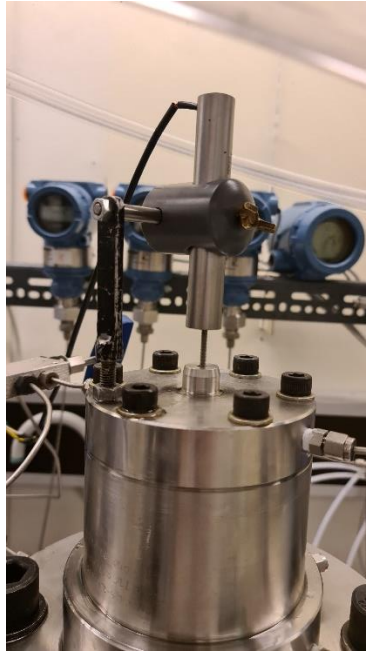
Figure 5: LVDT on top of the cell.

3.1.7 Brine cylinder

The previously described brine was flooded through the core using a brine cylinder. This cylinder contained the injection brine at the top end and distilled water (DW) at the bottom end, separated by a piston. The brine cylinder and triaxial cell are connected by metal tubing. As DW was pumped into the bottom of the cylinder at a given rate this would displace the piston, pushing the brine out into the tubing going to the cell at an equal rate by using a Gilson 307 pump. The brine needs to be refilled when empty. The brine cylinder is pictured in figure 6.
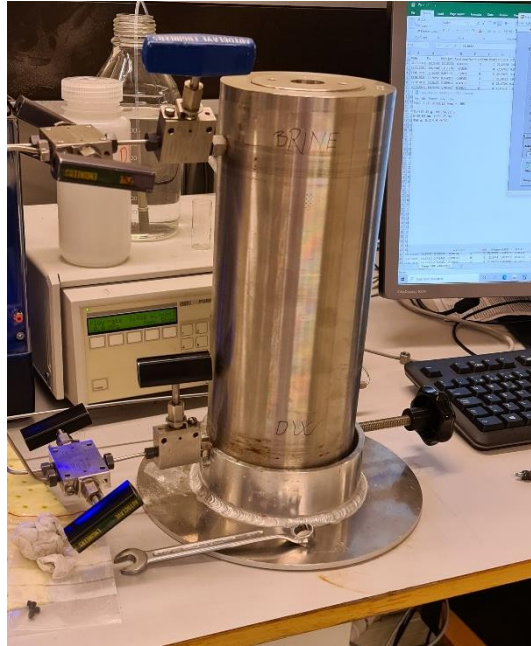
Figure 6: Brine cylinder with Gilson pump in the background

3.1.8 Pumps

A total of three pumps were needed per cell to carry out the experiment. Two pumps were used to maintain confining pressure and axial pressure and one was used flood the core. For the Stevns Klint setup, Vindum VP-series pumps were used for the confining pressure and axial pressure. The Kansas setup used Quizix QX-series pumps for the same purposes. The confining pump ensures that the confining pressure remains constant by pumping marcol 82 in or out of the cell as needed, while the axial pump pumps marcol 82 into the piston chamber moving the piston down onto the core and ensuring that the piston pressure remains constant. Both setups used a Gilson pump (307 High Performance Liquid Chromatography) for the core flooding.

3.1.9 Additional equipment

A back-pressure regulator is attached to the outlet tubing. This keeps the pore pressure stable. Additionally, there are four digital gauges of type Emerson Rosemount. These display the following parameters:

- Pore Pressure
- Differential pressure
- Piston pressure
- Confining pressure

3.2 Achieving testing conditions

For the experiment to yield any relevant results in terms of oil production, it had to be conducted at reservoir conditions. To achieve this the temperature had to be increased. The pressure was also increased, but not to reservoir conditions. The reason for this will be explained in the next section.

3.2.1 Confining/pore pressure

To achieve the correct confining pressure the pumps were used. First any remaining air was bled out by opening the confining valve at the top of the cell and pumping in marcol 82, pushing out the air and thereby filling up the confining chamber with marcol 82. Once this had been done the confining valve was closed again and pressure was built up. After reaching 0.5 MPa the core was injected with the brine, displacing the distilled water. After this the pore pressure and confining pressure was raised simultaneously, from 0 to 0.7 MPa and 0.5 to 1.2 MPa respectively. Confining pressure in the SK cell was later increased to 2.0 MPa. However, this was not done to the Kansas cell because of an oversight. When this error was detected, we chose to not increase the confining pressure 2.0 MPa, since this pressure difference would not have made a significant impact on chemical interactions (Nermoen et al. 2016). These pressures are far lower than what would be encountered in a real reservoir. The reason for why greater pressure is not used is to prevent the core from deforming. We need confining pressure primarily to prevent the brine from simply flowing between the core and the plastic sleave. The pore pressure is needed to prevent the brine from boiling inside the core because of the high temperatures. The pore pressure also counteracts the confining pressure, preventing too much deformation.

3.2.2 Piston pressure

The piston pressure was achieved by following similar steps as the increase of confining pressure. First the air was removed from both the upper and lower piston chambers through an

outlet valve. The upper piston outlet valve is then closed while the lower valve remains open, and the marcol starts pushing the piston down. This must be done slowly, as applying a hard and sudden pressure to the core can crack it, meaning the experiment must be terminated. During the lowering of the piston, the piston pressure is monitored carefully via LabVIEW. When the piston contacts the core the pressure will spike, at which point the piston is stopped manually by turning off the pump. The pump is then set to maintain a constant pressure of 0.6 MPa, a pressure which will be maintained for the duration of the experiment.

3.2.3 Heating

We are running two concurrent cells for this experiment, one at 100ºC (Stevns Klint) and one at 130ºC (Kansas). For both cells, a heating jacket is used to reach and maintain the desired temperatures. As the marcol 82 inside heats up it will naturally expand. To prevent this from increasing the confining pressure and damaging the core the excess is bled out through a spring valve. During the heating process the confining pump is switched off to prevent disruption of the heating by injection of cold oil into the confining chamber.

3.3   Flooding, sampling and analysis

3.3.1 Flooding

After all the aforementioned equipment had been assembled and all necessary preparations had been completed the actual flooding could begin. This is the main part of the experiment, where brine is actually being flooded through the core and made to interact with each other. The experiments start by flooding each core with 1 PV/day. Then, when steady state is determined to have been achieved at this rate, the flowrate is lowered to approximately 0.5 PV/day. Again, we wait until steady state has been achieved before lowering the flowrate further to approx. 0.25 PV/day. After this we will increase the flowrate to 2 PV/day, then 4, then 8 and then finally back to 1. This pattern of flooding will be used for both cores.

3.3.2 Sampling

The brine which had passed through the core would need to be sampled and then analyzed. This was done with a Gilson sampling machine (GX-271 Liquid Handler), and the samples were put into small vials. The time of each individual sampling was logged. The vials were weighed both before and after a sample was taken, such that the amount of liquid in them could be determined.

This could then be used to calculate the true flowrate, which could be compared to the planned flowrate. Sampling is done continuously throughout the experiment to ensure we have enough datapoints to accurately present our findings. At the start of both tests, six samples were collected every 24 hours for 2-3 days, as the number of reactions between the brine and the rock material were assumed to be higher during this first period. The number of samples taken were reduced to one every 24 hours as this initially high reactivity tapered off.

To avoid evaporation each vial was capped during sampling and as soon as possible after the sampling had been completed placed in a refrigerator. The combination of airtight caps and refrigeration is assumed to reduce evaporation to negligible levels.

3.3.3 Ion chromatography analysis

The effluent samples were analyzed with an ion chromatograph (Dionex Ion Chromatography System (ICS)-5000). The machine is highly sensitive, so the samples first had to be diluted 1000 times with nanopure water. This was done with a Gilson GX-271. After the samples had been diluted, they were transferred into smaller vials with a syringe. The syringe was tipped with 0.2-micron filter to get rid of any potential solids and oil.

Along with the actual samples discussed above, several "standard" samples were also entered into the IC-machine. These were:

- The original brine (0.219 M MgCl2)
- Synthetic seawater (SSW)
- 0.2 M MgCl2 + 0.013 M CaCl2

This is because the machine cannot give the actual concentration but rather a signal area for each ion. The ion concentration for the standard samples were known and could therefore be used to calculate the concentration of the actual samples.

3.4 The mathematical model

The goal of this thesis is to see if a mathematical model can be used to fit gathered experimental data from injection of $MgCl_2$ brine into a calcite core, as well as possibly predict the results of future experiments. Assuming we have a perfect substitution between ions (Mg-Ca2) MATLAB can be used to model this by using a built in function called cftool. The model presented in this

section is based on the one presented by (Andersen & Berawala, 2019). As the previously described brine is injected a substitution reaction between the Mg^{2+} and Ca^{2+} will begin. This will cause the dissolution of Calcite ($CaCO_3$) and precipitation of Magnesite ($MgCO_3$).

The reaction rate at which this happens is assumed to be:

$$\dot{r} = k_1 \left(C_{Mg} - k_2 C_{Ca} \right)^n \quad (6)$$

Here $k_1 \left[\dfrac{1}{\left(\frac{mol}{m^3} \right)^{n-1}} \dfrac{}{s} \right]$ is a rate coefficient, k_2 is a dimensionless reaction constant and n is the dimensionless reaction order. When the reaction reaches equilibrium, $\dot{r}$ is equal to zero. Using this to solve equation (6) for k_2 gives:

$$k_2 = \frac{C_{Mg}^{eq}}{C_{Ca}^{eq}} \quad (7)$$

The value of k_2 varies with temperature but remains fixed at any given stable temperature. This is true regardless of the concentration of the injected brine. Knowing this, only the rate coefficient (k_1) and reaction order (n) will be modified and tested to get a function matching as closely as possible the gathered experimental data.

Given the substitution reactions between the calcium and magnesium the sum of the concentrations is conserved and identical to the injected value. We can therefore write:

$$C_{Ca}(x) + C_{Mg}(x) = C_{Ca}^{inj} + C_{Mg}^{inj} \quad (8)$$

Here x is the position in the chalk core and C^{inj} denotes the ion concentrations of the injected brine.

At steady state we get the following transport equations for the reaction rate:

$$d_x(v_w C_{Ca}) = \dot{r} \quad (9)$$

$$d_x(v_w C_{Mg}) = -\dot{r} \quad (10)$$

Here v_w is the pore velocity. Due to the substitution behavior discussed earlier the reaction rates

have equal magnitude but opposite direction. To solve the transport equations the reaction rate from (6) is used. As equation (8) states, the concentration at x is constant and equal to the concentration of the ejected brine. To solve (9) for the case where n = 1, equation (6) is rewritten as

$$\dot{r} = k_1\left(C_{Ca}^{inj} + C_{Mg}^{inj} - (1 + k_2)C_{Ca}\right) \quad (11)$$

Let

$$A = C_{Ca}^{inj} + C_{Mg}^{inj}, \qquad B = 1 + k_2, \qquad \forall x \in [0, L] \quad (12)$$

Giving us

$$\frac{dC_{Ca}}{dx} = \frac{k_1}{v_w}(A - BC_{Ca}) \quad (13)$$

Giving the following solution of C_{Ca}:

$$C_{Ca}(x) = \frac{A}{B} + c_1 e^{-B\frac{k_1}{v_w}x} \quad (14)$$

Here, c_1 is some constant found from the boundary conditions $C(x) = C^{inj}$. We now insert the original variables for A and B, getting

$$C_{Ca}(x) = \frac{C_{Ca}^{inj} + C_{Mg}^{inj}}{1 + k_2} + c_1 e^{-(1+k_2)\frac{k_1}{v_w}x} \quad (15)$$

Defining the calcium concentration at equilibrium (C_{Ca}^{eq}) and a dimensionless Dahmköhler number, when n = 1, as

$$C_{Ca}^{eq} = \frac{C_{Ca}^{inj} + C_{Mg}^{inj}}{1 + k_2} \quad (16)$$

$$N_{Da,1} = (1 + k_2)\frac{k_1 L}{v_w} \quad (17)$$

and c_1 as

$$c_1 = -\left(C_{Ca}^{eq} - C_{Ca}^{inj}\right) \quad (18)$$

gives us equation (9) in the following form:

$$C_{Ca}(x) = C_{Ca}^{eq} - (C_{Ca}^{eq} - C_{Ca}^{inj})e^{-N_{Da,1}\frac{x}{L}} \quad (19)$$

For magnesium we have the equilibrium concentration as:

$$C_{Mg}^{eq} = \frac{k_2(C_{Ca}^{inj} + C_{Mg}^{inj})}{1 + k_2} \quad (20)$$

Equation (10) similarly becomes

$$C_{Mg}(x) = C_{Mg}^{eq} - (C_{Mg}^{inj} - C_{Mg}^{eq})e^{-N_{Da,1}\frac{x}{L}} \quad (21)$$

In cases where $n \neq 1$, equation (19) and (20) becomes

$$C_{Ca}(x) = C_{Ca}^{eq} - (C_{Ca}^{eq} - C_{Ca}^{inj})\left[1 + \left(\frac{C_{Ca}^{eq} - C_{Ca}^{inj}}{C_{Mg}^{inj} - k_2 C_{Ca}^{inj}}\right)^{n-1} N_{Da,n}\frac{x}{L}\right]^{\frac{1}{-n+1}} \quad (22)$$

$$C_{Mg}(x) = C_{Mg}^{eq} - (C_{Mg}^{inj} - C_{Mg}^{eq})\left[1 + \left(\frac{C_{Mg}^{inj} - C_{Mg}^{eq}}{C_{Mg}^{inj} - k_2 C_{Ca}^{inj}}\right)^{n-1} N_{Da,n}\frac{x}{L}\right]^{\frac{1}{-n+1}} \quad (23)$$

respectively, and $N_{Da,n}$ becomes

$$N_{Da,1} = (1 + k_2)^n \frac{k_1 L}{v_w}\left(C_{Mg}^{inj} - k_2 C_{Ca}^{inj}\right)^{n-1}(n - 1) \quad (24)$$

With these equations we can start modelling in MATLAB with varying values for k_1 and n, and thus make a theoretical model which matches with the observed values from the experiments.

4 Results

As stated earlier, the results were measured using an Ion Chromatography machine and then plotted into excel to get presentable values.

4.1   Experimental findings

Section 4.1 will present the results as they were found, while the results of the modeling will be shown in section 4.2.

4.1.1 Reactions

The expected results of the floodings are a substitution reaction between magnesium and calcium, achieved by the dissolution of calcite and the precipitation of magnesium. This is described by the following two reactions:

$$CaCO_3 \leftrightarrows Ca^{2+} + CO_3^{2-}$$

$$Mg^{2+} + CO_3^{2-} \leftrightarrows MgCO_3$$
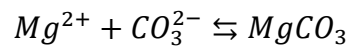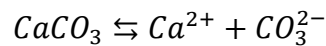
The concentrations of ions in the measured effluents will reflect the increase in magnesium and decrease in calcium content that the core experiences. Any magnesium missing from the brine can then reasonably be assumed have substituted with the calcium present in the core, based on the measured effluents. Using these measuring points, plots will be created to illustrate how the reactions behave over time with changing flowrates.

4.1.2 SKA3 Rate Tests

As we began the flooding, we initially started flooding with a flowrate of one pore volume per day (PV/day), then lowered this to ca. 0.5 PV/day, and then again lowered this to ca. 0.25 PV/day. This will be referred to as the first phase of the experiment. In the second phase we will increase the flowrate. We split the results into two phases to be discussed separately in order to keep the results section more clear.

We started the experiment by flooding the Stevns Klint core (SKA3) at 1 PV/day. This worked out to 0.026 ml/min. After less than a day of flooding, peak concentration of calcium had been reached. The calcium concentration was at 0.0367 mol/L at this stage. The concentrations then quickly started leveling off, moving towards steady state, Fig 7. Flooding was continued until day 37 to ensure that the concentrations had stabilized, at which point the calcium concentration was 0.0055 mol/L and magnesium was 0.2149 mol/L.
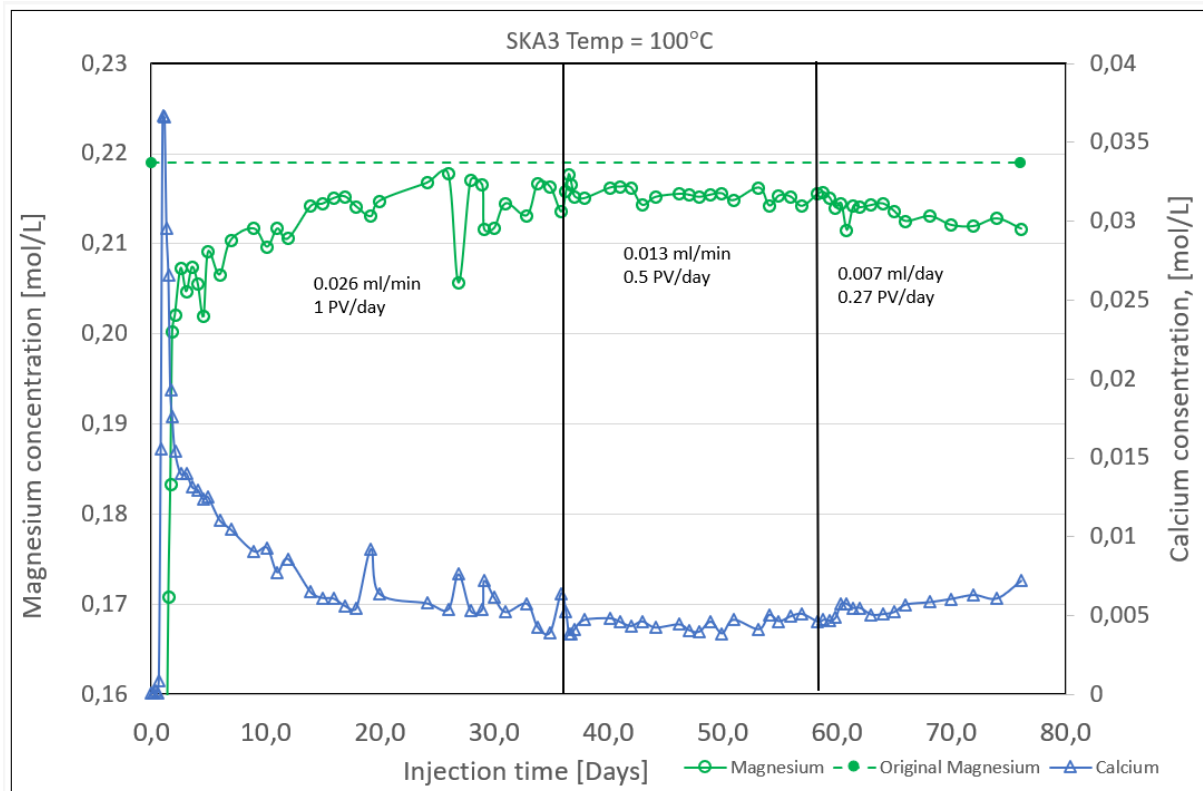
Figure 7: Mg and Ca levels for SKA3 at 100°C with 0.219 M MgCl$_2$ injected. The core is a Stevns Klint core.

The average concentrations for each of the flowrates for the first phase is shown in table 2. The flowrates are calculated by averaging the last few effluent concentrations measured when the reactions are assumed to have reached steady state. This is true for all subsequent tables dealing with average concentrations.

Table 2: Average concentrations of Magnesium and Calcium for SKA3 during first phase.

	1 PV/day	0.5 PV/day	0.27 PV/day
SKA3 (Mg)	0.2149 mol/L	0.2147 mol/L	0.2121 mol/L
SKA3 (Ca)	0.0051 mol/L	0.0043 mol/L	0.0064 mol/L
Std. deviation (Mg)	0.0016	0.0006	0.0005
Std. deviation (Ca)	0.0012	0.0002	0.0005

The concentrations seen in the table above does not fully meet the expected behavior of lowering the flowrate. When going from 1 to 0.5 PV/day the magnesium concentration decreases very slightly, by 0.0002 mol/L. The calcium concentration decreases by 0.0008 mol/L. The change in magnesium between these two flowrates is too small to be considered significant, though the calcium is. However, given the fact that the concentration of calcium is going down even though it should have gone up when the flowrate was lowered gives us reason to question this result. In any case, based on the data we can conclude that interaction between the brine and core did not increase significantly. From 0.5 to 0.27 PV/day we see more interaction between the core and brine with a decrease of 0.0026 mol/L and increase of 0.0023 mol/L for magnesium and calcium, respectively.

After lowering the flowrate to just 0.25 PV/day, we started flooding with higher flowrates than 1 PV/day. The rate was increased up to 2 PV/day, and then doubled each time until the flowrate reached 8 PV/day. Finally, it was decreased to 1 PV/day. The evolution of the flowrate in PV/day was therefore $0.25 \rightarrow 2 \rightarrow 4 \rightarrow 8 \rightarrow 1$. The lowering of the flowrate to 1 PV/day was the final change in flowrate which will be discussed in this thesis. This period of increasing and then lowering the flowrate again will be referred to as the second phase of the experiment. The trends of the second phase are shown in figure 9.
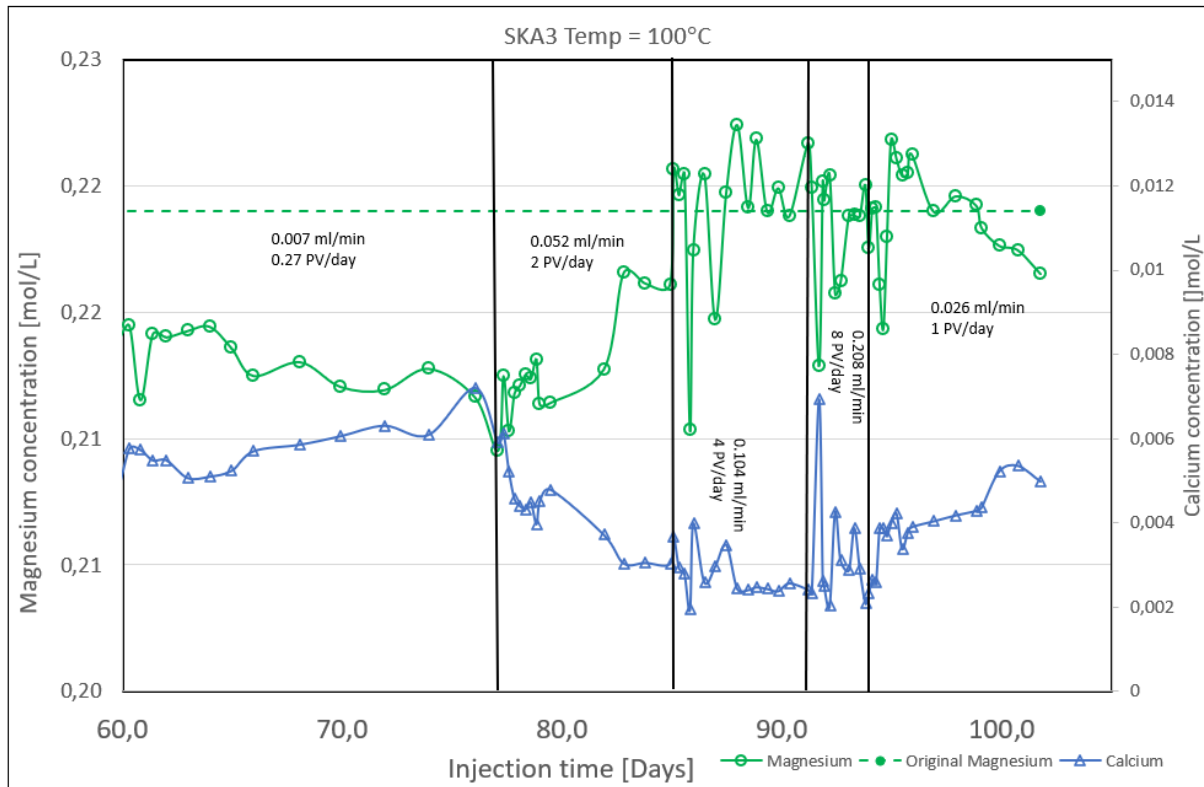
Figure 9: SKA3 magnesium and calcium concentrations plotted - Second Phase.

The average concentrations of ions measured in the effluents is presented in table 3. The averages follow the expected pattern to some extent. When the flowrate is increased from 2 to 4 PV/day magnesium concentration goes from 0.2163 to 0.2192 mol/L an increase of 0.0029 mol/L. Calcium only decreases by 0.0005 mol/L at the same point, almost 6 times less change than magnesium experienced. Between 4 and 8 PV/day magnesium changed by only 0.0001 mol/L less than the standard deviation. The calcium concentration changed more at this point than magnesium, increasing by 0.0004 mol/L. This is beyond one standard deviation, but it is in the opposite direction from what was expected. Given that the magnesium concentration hardly moved we can assume that there are no real changes to the interaction between the brine and the core when increasing flowrate from 4 to 8 PV/day. When lowering the rate down to 1 PV/day we see a decrease in magnesium concentration of 0.0016 mol/L and an increase in calcium concentration of 0.0031 mol/L.

Table 3: Ion concentrations for SKA3 during the second phase.

	2 PV/day	4 PV/day	8 PV/day	1 PV/day

SKA3 (Mg)	0.2163 mol/L	0.2192 mol/L	0.2191 mol/L	0.2175 mol/L
SKA3 (Ca)	0.0030 mol/L	0.0025 mol/L	0.0029 mol/L	0.0050 mol/L
Std. deviation (Mg)	0.0003	0.0006	0.0028	0.0007
Std. deviation (Ca)	0.00001	0.0001	0.0017	0.0004

The concentration results of this core suggests that at a temperature of only 100ºC the flowrate does not significantly impact the concentrations of ions in the effluents.

4.1.3 KR30 Rate Tests

The Kansas core (KR30) flooding followed the same pattern as the aforementioned SKA3 core. Measured calcium levels in the effluents started increasing rapidly just before two days had passed and peaked at two days, before also decreasing to steady state, Fig 8. We see a lot more interaction take place between the brine and the chalk here compared to the SKA3 test. This is as a result of the higher temperature of this test.
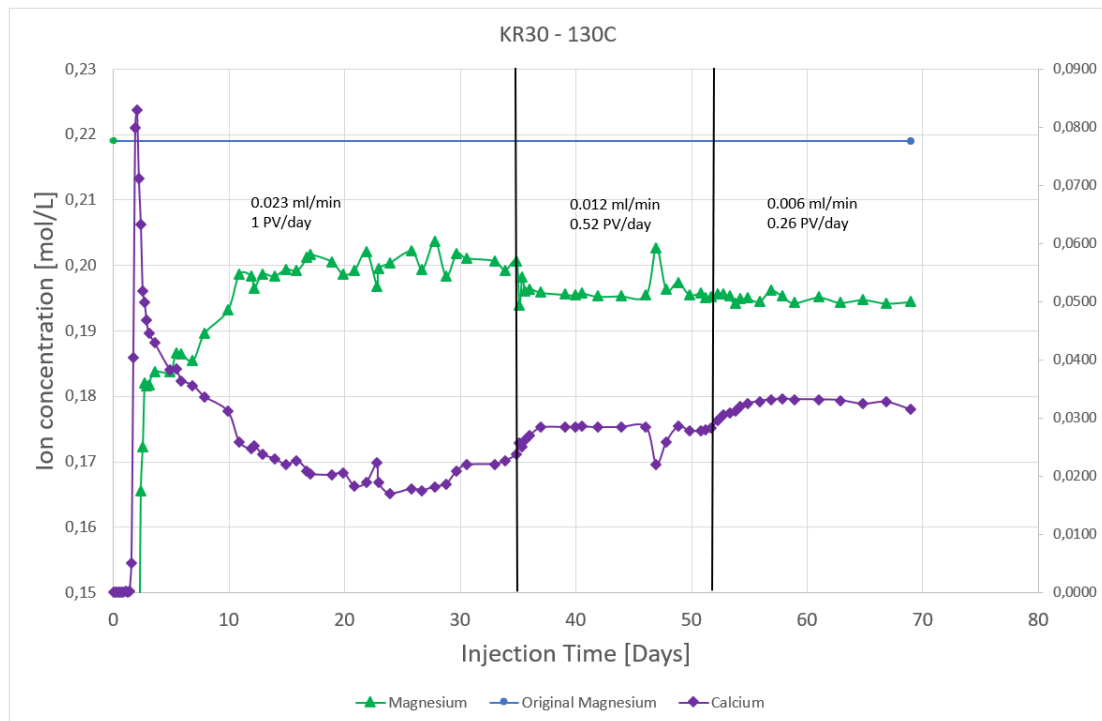

Figure 8: Mg and Ca levels for KR30 at 100°C with 0.219 M MgCl$_2$ injected. The core is a Kansas core.

The average concentrations for each flowrate for each core are given in the following table (table 3):

Table 4: Ion concentrations at equilibrium for KR30 during first phase of the experiment.

	1 PV/day	0.5 PV/day	0.26 PV/day
KR30 (Mg)	0.2008 mol/L	0.1963 mol/L	0.1944 mol/L
KR30 (Ca)	0.0219 mol/L	0.0275 mol/L	0.0324 mol/L
Std. deviation (Mg)	0.0011	0.0009	0.0002
Std. deviation (Ca)	0.0007	0.0011	0.0007

For the core KR30 being run at 130ºC we see significantly bigger changes in concentrations when lowering the flowrate, as well as much higher levels of precipitation in general. We also see that the concentrations change in the expected manner. Between 1 PV/day and 0.5 PV/day the calcium concentration increases by 0.0056 mol/L, from 0.0219 to 0.0275 mol/L. Between 0.5 and 0.26 PV/day it increases by 0.0049 mol/L, from 0.0275 to 0.0324 mol/L. However, the problem noted in the table of SKA3 shows up here as well, namely the fact that the calcium concentration increases more than the magnesium rises. From 1 PV/day to 0.5 PV/day the magnesium concentration goes from 0.2008 to 0.1963 mol/L, a reduction of just 0.0045 mol/L. This trend continues when lowering the flowrate from 0.5 to 0.26 mol/L, where the reduction in concentration is just 0.0019 mol/L. The fact that this is recurring seems to suggest it is not just a measuring error or some other anomaly, but a more systematic occurrence. The results of (Olsen A.T., 2020) saw a similar result. When going from 1 to 0.5 PV/day calcium increased from a concentration of 0.023 to a concentration of 0.028 mol/L, a net increase of 0.005 mol/L. Magnesium only decreased by 0.002 mol/L in the same period. When going from 0.5 to 0.25 PV/day calcium increased by 0.004 mol/L while magnesium decreased by only 0.001 mol/L. Both tests therefore show a tendency to lose more calcium than they gain magnesium. However, we can see that core KR30, under comparable testing conditions as core SKA1 gives higher concentrations of both calcium and magnesium. This is possibly a result of the impurities in core KR30 as (Madland et al., 2010) found that the presence of silicates increases the

precipitation of magnesium, because the magnesium also forms minerals with the silicates. It is possible that at such low flowrates some of the chalk simply dissolves into the water without any interaction with the $MgCl_2$ suspended in the brine. As described earlier, the brine is mixed to equilibrium with $CaCO_3$ before the $MgCl_2$ is added. This is done to make the water more inert, meaning it should not react with the chalk on its own like this.

KR30 during the second phase went through the same pattern of increasing and then later decreasing the flowrate as described in 4.1.4 and gave us the following plot (Fig 10).
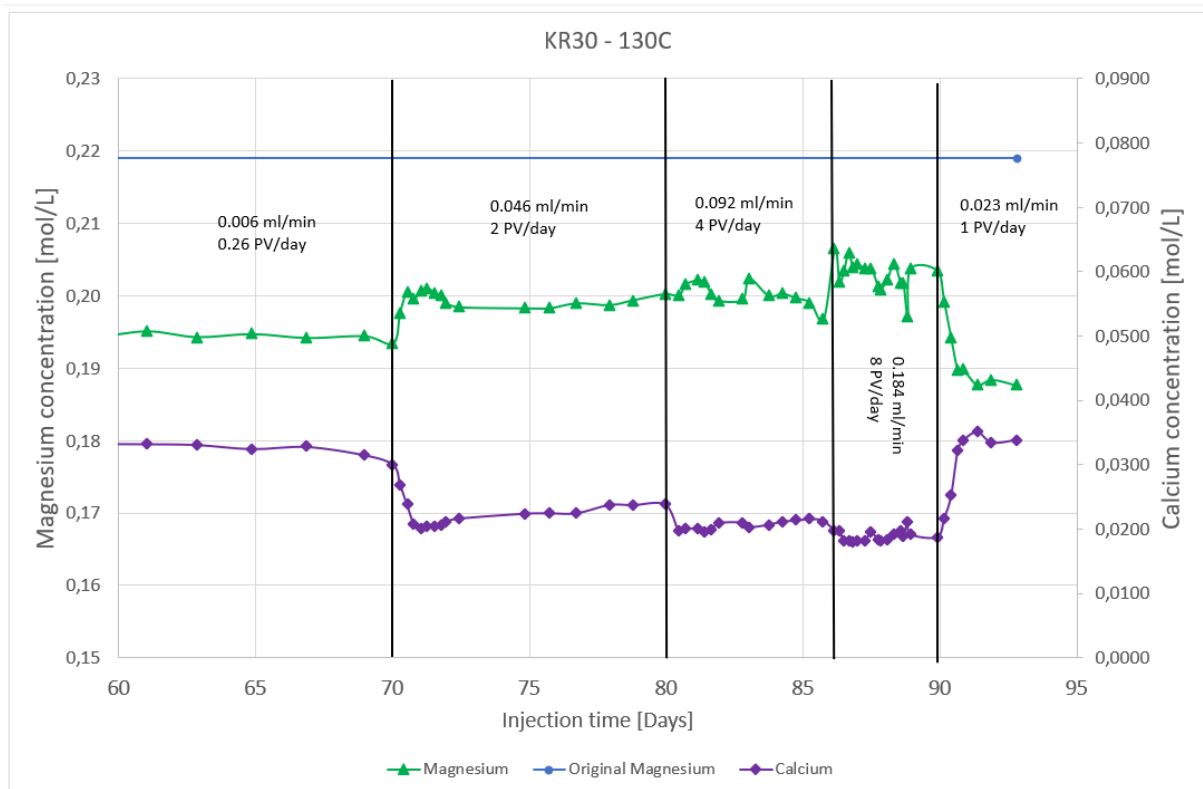

Figure 10: KR30 magnesium and calcium concentrations plotted - Second Phase.

Just from looking at the plot we can already see a much clearer correlation between the expected behavior and the actual measured results. When the flowrate is increased from 0.26 PV/day to 2 PV/day a clear and immediate reduction in the number of reactions occurs. This is also the case for both additional increases in flowrate. When the flowrate is lowered to 1 PV/day at the end, the interaction between the brine and chalk becomes more intense again and far more calcium is found in the effluent samples. The plotted data also clearly indicates that steady state was achieved, as it shows the reactions quickly stabilize towards a certain concentration over the course of 1-2 days before remaining stable until the flowrate is changed again. The precise

values for the concentrations are found in table 5.

Table 5: Ion concentrations for KR30 during the second phase.

	2 PV/day	4 PV/day	8 PV/day	1 PV/day
KR30 (Mg)	0.1989 mol/L	0.1998 mol/L	0.2011 mol/L	0.1884 mol/L
KR30 (Ca)	0.0231 mol/L	0.0212 mol/L	0.0197 mol/L	0.0341 mol/L
Std. deviation (Mg)	0.0005	0.0005	0.0028	0.0010
Std. deviation (Ca)	0.0007	0.0004	0.0010	0.0007

The values from the table reinforces the impression gained from looking at the plot, clearly showing the expected behavior of decreasing and increasing the flowrate. When increasing the flowrate from 2 to 4 PV/day the magnesium increases by 0.0009 mol/L and calcium decreases by 0.0019 mol/L. When going from 4 to 8 PV/day magnesium increases by 0.0013 mol/L and calcium decreases by 0.0015 mol/L. We can see that there is greater variation in how much the concentrations changes. Finally, when lowering back down to 1 PV/day the concentrations changed dramatically. The magnesium concentration fell by 0.0127 mol/L and the calcium concentration increased by 0.0144 mol/L. Compare this to the initial concentrations which were 0.2008 and 0.0219 mol/L for magnesium and calcium respectively. This illustrates a phenomenon which was shown during earlier tests, namely the tendency for the same flowrate to give different concentrations of magnesium or calcium based on which flowrate was used before.

4.2 Modelling

The model described in the theory section of this thesis gives you the concentration at any given position x between the inlet and outlet of a chalk core being flooded. Every effluent sample taken for the duration of this experiment has been taken from the outlet. This is because we are not interested in seeing how position in the core affect ion concentration, but rather how the flowrate affects it. This means that $\frac{x}{L} = 1$, allowing equations (22), (23) and (24) to be expressed by flowrate instead as x is now constant.

4.2.1 Model parameters

In this model we will be altering three different parameters to modify our model and fit it to the experimental data. These are:

- The reaction order, n
- The first rate coefficient, k_1
- The second rate coefficient, k_2

By keeping two of these parameters fixed while modifying the third we can illustrate the effect this specific parameter has on the model. Setting $k_2 = 6$ and $k_1 = 5.7223 \times 10^{-8}$, the reaction order *n*, an exponent, was plotted between 0.2 and 7.4 with intervals of 0.3. These parameters were chosen as they were the same that Andre Tvedt Olsen had chosen in his BSc (Olsen, A. T., 2020) to illustrate the behavior of the plots when using different parameters. This experiment is carried out at similar conditions and it is therefore fitting to use these values here as well. At reaction orders higher than 7.4 the model expects equilibrium to be achieved independently of the velocity when said velocity is between 0.25 and 16 PV/day. With reaction order lower than 0.2 virtually no reactions take place over the same velocities, the concentrations of magnesium and calcium remaining constant. This behavior is illustrated in figures 11 and 12, figure 11 showing calcium and figure 12 showing magnesium. We can say that the reaction order n determines the reaction kinetics of the reaction. Increased n means increased reaction kinetics; decreased n means decreased reaction kinetics. This behavior is true for any values of k_1 and k_2.
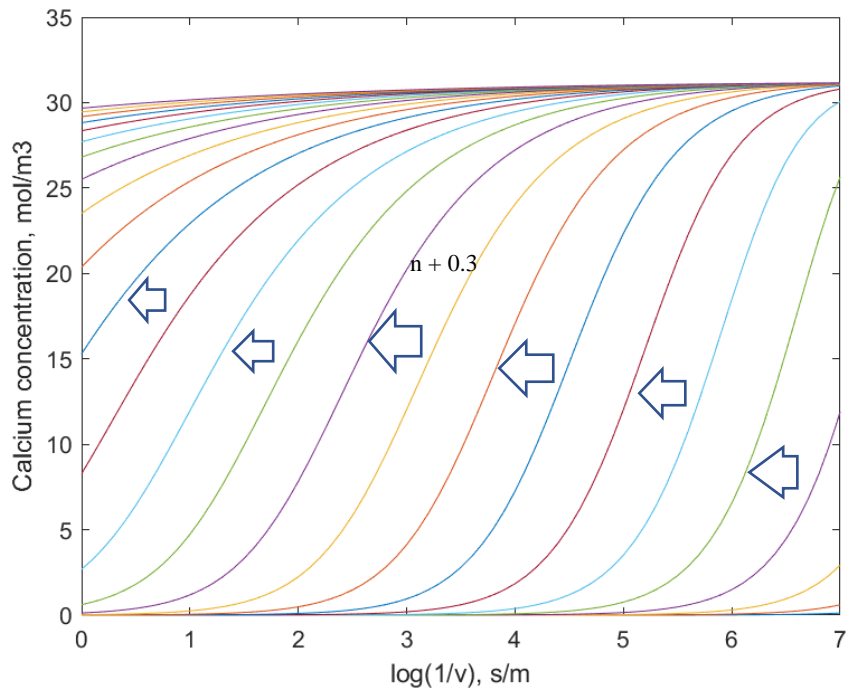
Figure 11: The effect of varying n on the model. The graph moves from right to left as n increases. This means that a higher value of n means that reactions reach equilibrium faster.
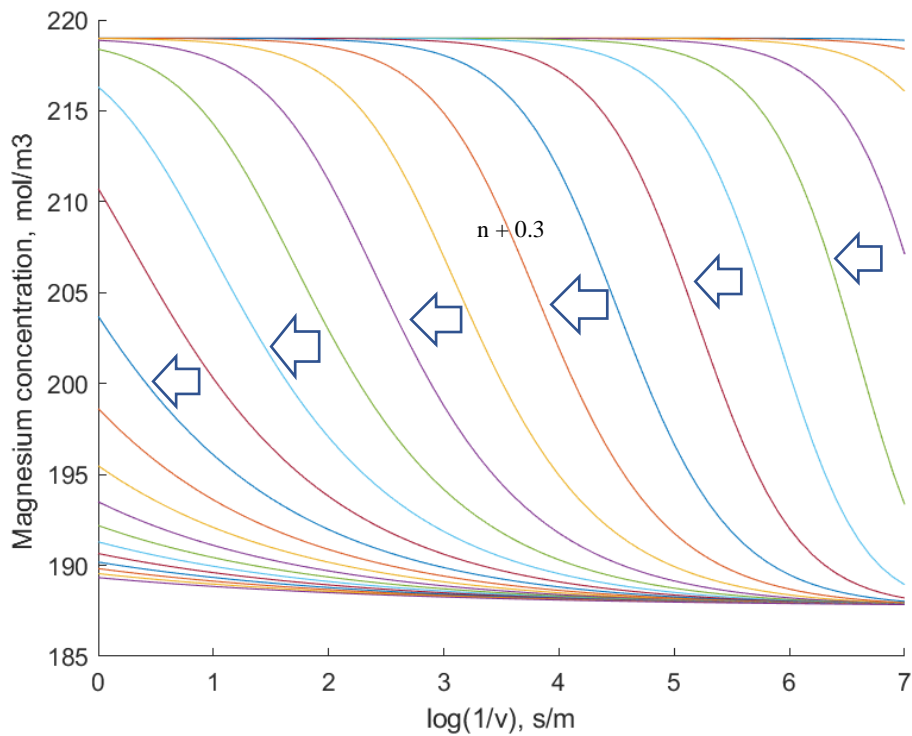

Figure 12: The behavior of n is the same as in figure 9 but opposite for Mg. Graph moves from right to left as n increases.

The first rate coefficient k_1 affected the model in much the same way as the rate coefficient n.

When k_1 is at a high or low value equilibrium is achieved rapidly and independently of injection velocity, though the values producing these results are further apart than the values of n producing the same results. Maximum and minimum concentrations are however unaffected by the value of both k_1 and n, as the equilibrium concentration is only dependent on k_2 among the parameters we are varying.

When k_2 is decreased, the equilibrium concentration is increased, and vice versa. It also affects the reaction kinetics, though to a lesser degree than the other parameters. This parameter forms a part of the denominator in the equilibrium equations (11) and (15), meaning that this behavior is to be expected. This behavior is illustrated in figures 13 and 14.
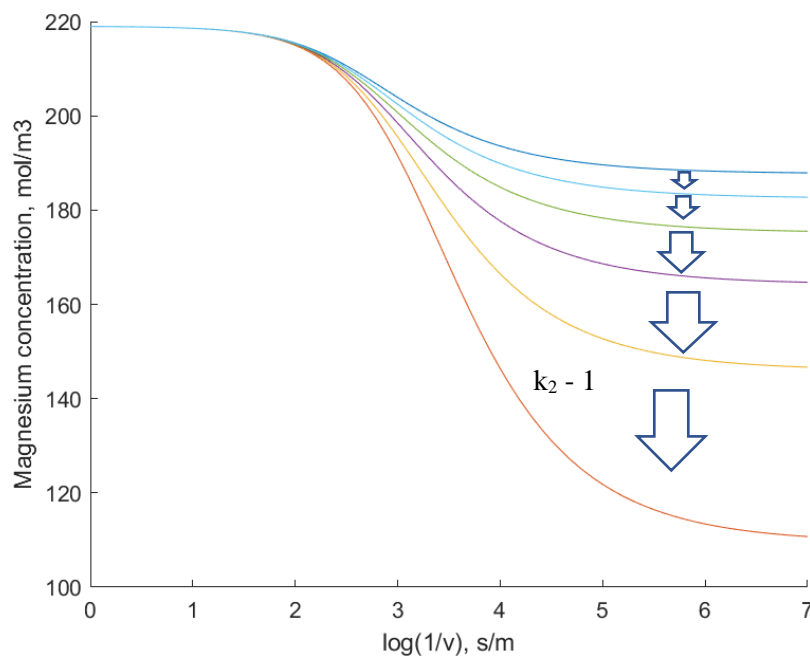

Figure 13: Effect of k2 on magnesium conc. Lower k2 shifts the graph down because it decides the relation between the equilibrium constants.
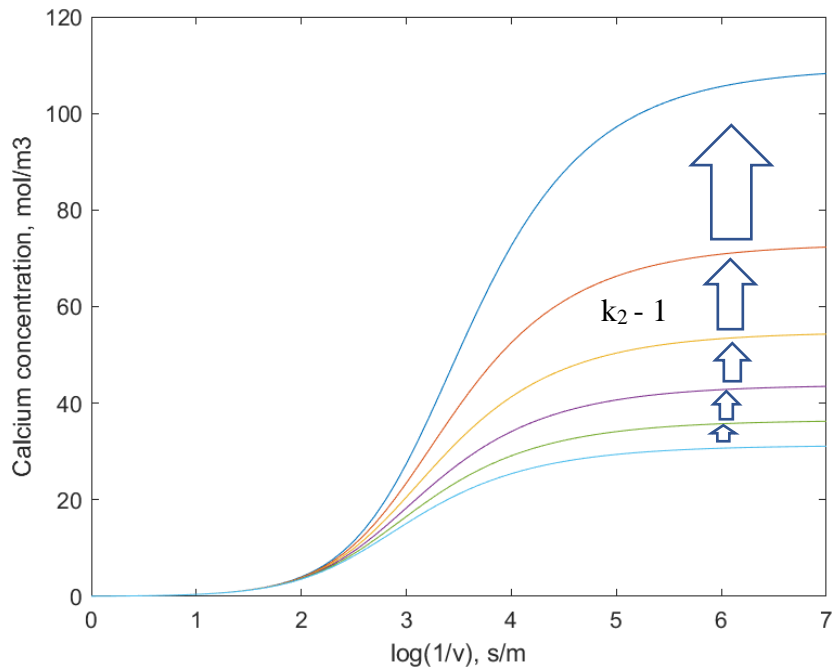
Figure 14: Effect of k2 on calcium conc. Lower k2 shifts graph up.

4.2.2 SKA3 results compared to the model

In order to find fitting values for k_1 and k_2 to use when fitting the model to the experimental results, we can use the following approach. By using what is known as a "curve fitting tool" available through MATLAB we can find reasonable values to apply to k_1, k_2 and n by inputting our experimental results and then inputting the formula for concentration discussed in section 3.4. By setting all the steady state concentrations we have measured as a vector, both for calcium and magnesium in the same vector we are able to get the parameters used to fit both at the same time. For core SKA3 we get the following results:
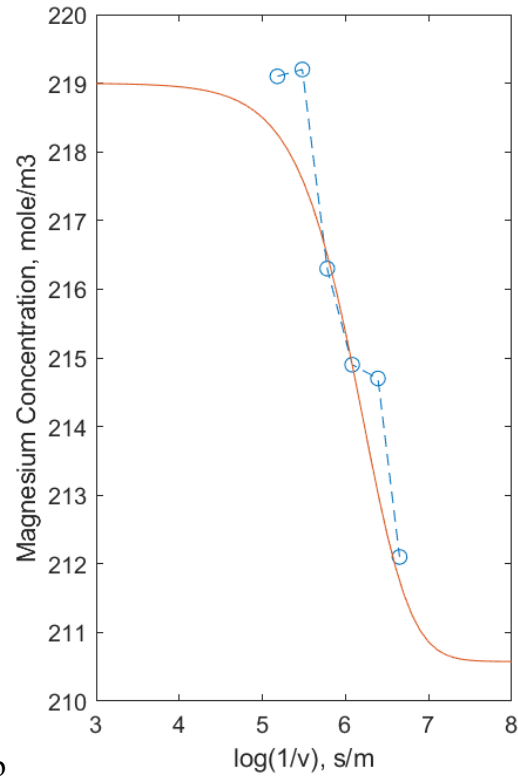
- n = 1.413
- k_1 = 4.64e-08
- k_2 = 29.05

Setting these values as our parameters in the plot gives us the curves shown in Fig. 15a and b:

a

b
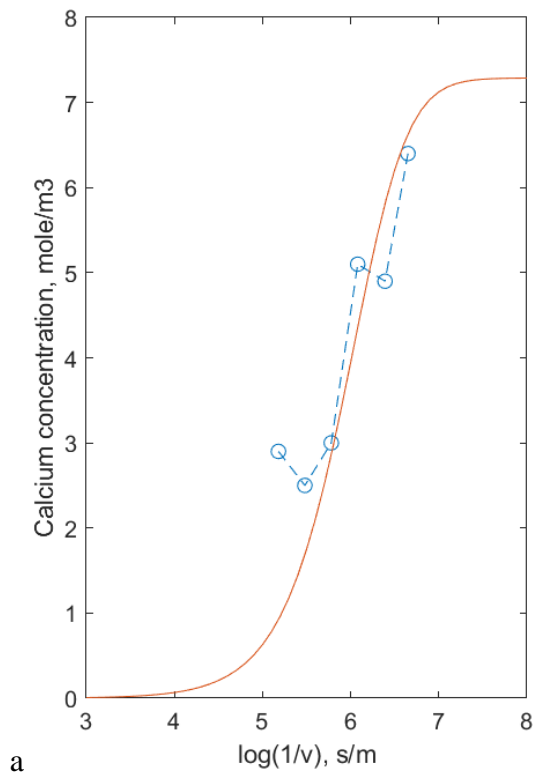
Figure 15a: Fitted curve for SKA3 Ca conc.   *Figure 15b: Fitted curve for SKA3 Mg conc.*

To fit this curve in an appropriate manner we manually adjusted k_2 to extend the equilibrium points up for calcium and down for magnesium. The first curve found with the curve fitting tool started moving towards equilibrium to early, suggesting that the concentrations would reach equilibrium earlier than what the experimental data told us. By lowering k_2 we have lowered the reaction kinetics, which seems to more accurately illustrate the behavior suggested by the experimental data.

4.2.3 KR30 results compared to the model

The curves for core KR30 were acquired using the same program as core SKA3, but with a slightly different methodology. The curve fitting tool struggled to find a solution which fitted to every experimental datapoint. To fix this, the model was first approximated by manually manipulating the parameters until the model fit the measured data to a satisfactory degree. Then, a range of values was set for the parameters which included these approximated parameters. The program was then run again to finetune the parameters to a value within the previously explained range. This gave us the curve in figure 16a and b.
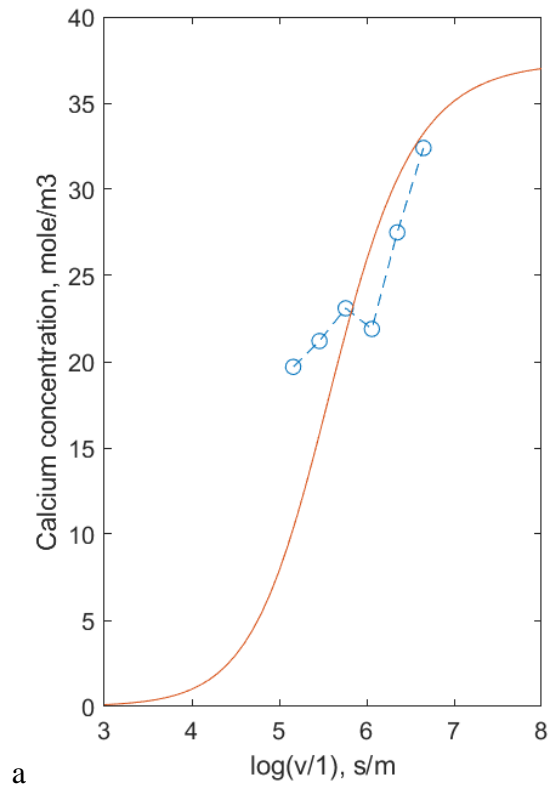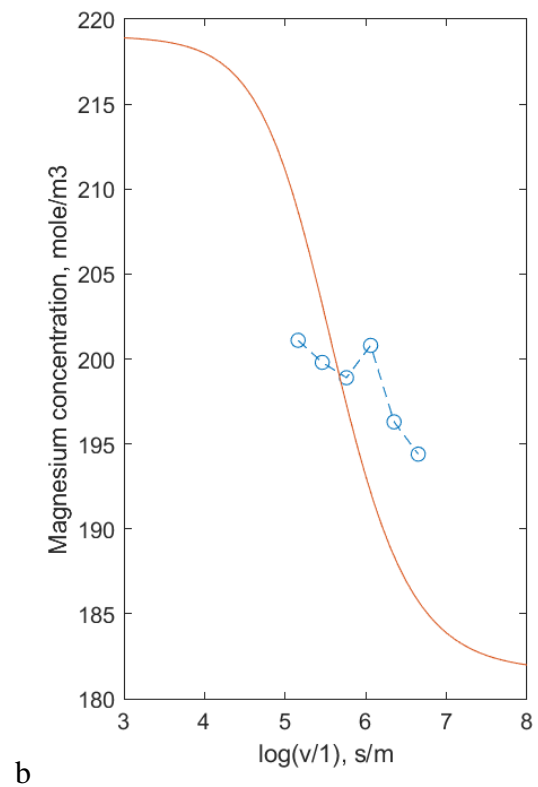
a

Figure 16a: Fitted curve for KR30 Ca conc.

b

Figure 16b: Fitted curve for KR30 Mg conc.

The values used to tune the model were:

- $k1 = 6.304\mathrm{e}{-08}$
- $k2 = 4.858$
- $n = 2.283$

The model was tuned by setting all the measurements as one vector in order to find the correct parameters for both the calcium and magnesium concentrations simultaneously. From looking at the model we can see that it fits the calcium concentrations better than the magnesium concentrations, with the tuned model not passing through the magnesium datapoints very well. Since we have a substitution reaction, we expect to see the magnesium and calcium concentrations change the same amount but in opposite directions. This did not happen in this case however, where we can see that calcium generally changes more, especially for the last three values.

5 Discussion

This section will discuss various elements of the experiment. What the results showed and what they might mean, how they relate to what has been found before and how more reliable and

logical results might be obtained in future tests.

5.1 Sources of error

The possibility for errors occurring during an experiment can never be truly avoided no matter how carefully one prepares. This section will discuss some possible errors encountered during this particular experiment, arising from either the way the results were measured or how the experiment in and of itself was carried out in terms of its procedures.

5.1.1 Failure to reach steady state

When analyzing the results from SKA3 in excel, we see a tendency for the concentration of calcium in the effluents to keep going down despite the flowrate having been lowered, with an equal though opposite response from the magnesium. The expected behavior, as mentioned earlier, is that when the flowrate is lowered the interaction between the brine and the chalk should increase. If the reactions truly do increase, we would see a jump in the amount of calcium in the effluents. The fact that we do not see an increase in the amount of calcium when lowering the flowrate suggests that the chemical interactions had not yet reached steady state. There exists a possibility that these irregularities could stem from contamination or experimental variations but given the systemic nature of these measurements returning unstable values we concluded that the effluents likely had not reached steady state. In the SKA3 setup the flowrate was lowered for the first time after 36 days when it was reduced from 1 PV/d to 0.5 PV/d. The fact that the reactions were not at steady state after flooding for so long suggests that at this temperature ($100°C$) achieving steady state takes an exceedingly long time. We had in excess of 4 months to conduct the experiments for this thesis, so due to time constraints we were at a certain point forced to change the flowrate to have the necessary amount of time left to get through the other flowrate-changes. If more time had elapsed, it is more probable that a steady state could have been reached.

The results found in the case of core SKA3 tended to show little activity between the brine and chalk, and often behaved in a very unexpected manner. For instance, when the flowrate was lowered from 1 PV/day to 0.5 PV/day (presented in section 4.1.2) we see a decrease in the activity between the brine and the core. When the brine spends a longer time in the core we naturally expect the opposite to occur, that is, an increase in reactions between brine and core. We can see that as magnesium increases, calcium decreases. This is the expected behavior given

that we have substitution. It is also possible that these measured concentrations are a result of an error in the dilution process. The sampled effluents are supposed to be diluted 1000 times, so the margins for error are slim. In any case, given how slight these changes are this is not enough to be a decisive result. The magnesium concentration at 0.5 PV/day falls within one standard deviation of the average concentration of 1 PV/day. The calcium concentration at 0.5 PV/day does not fall within one standard deviation of the average concentration of 1 PV/day. We can still conclude however that the lowered flowrate had a negligible impact on the interaction between the brine and the core. At 0.25 PV the concentration of magnesium falls enough to be significant, but the calcium concentration does not rise as much as the magnesium falls. Considering that the substitution of magnesium and calcium is the only reaction that is supposed to take place between brine and the core this is unexpected. For core KR30 the results were generally far more reasonable, and they will therefore not be discussed at length here.

5.2 Comparisons

In this section we will compare the results we got to the results obtained by (Olsen A.T, 2020). The experimental combinations are shown in table 6. We are most interested in seeing how much variations in temperature and chalk type affects the behavior of the reactions, so we will mostly be comparing our results with the results of core SKA1 as this uses the same brine concentration as we did.

Table 6: Experimental combinations for this experiment (2021) and the experiments of Olsen A.T, 2020

	Chalk type	Temp	Brine
SKA3 (2021)	Stevns Klint	100ºC	0.219 M $MgCl_2$
KR30 (2021)	Kansas	130ºC	0.219 M $MgCl_2$
SKA1 (2020)	Stevns Klint	130ºC	0.219 M $MgCl_2$
SKA2 (2020)	Stevns Klint	130ºC	0.0445 M $MgCl_2$

5.2.2 Comparison with earlier tests - Temperature

As mentioned in the introduction of this thesis a similar experiment of flooding chalk cores was carried out in 2020. These tests had an identical setup and tested two SK cores (SK1 and SK2), from the same block as SKA3, at the same temperature (130°C) but with different brines (0.219 and 0.0445 M MgCl$_2$). Our tests used one SK core (SKA3) at 100°C and one Kansas core (KR30) at 130°C but both used the same brine. How temperature affected reactions will be shown in this section, how chalk type affected it will be shown in the next. The averages were calculated using the last 3-4 measured concentrations before a flowrate change. The plots for both cores will be presented in the same figure (fig. 17) and compared to each other:
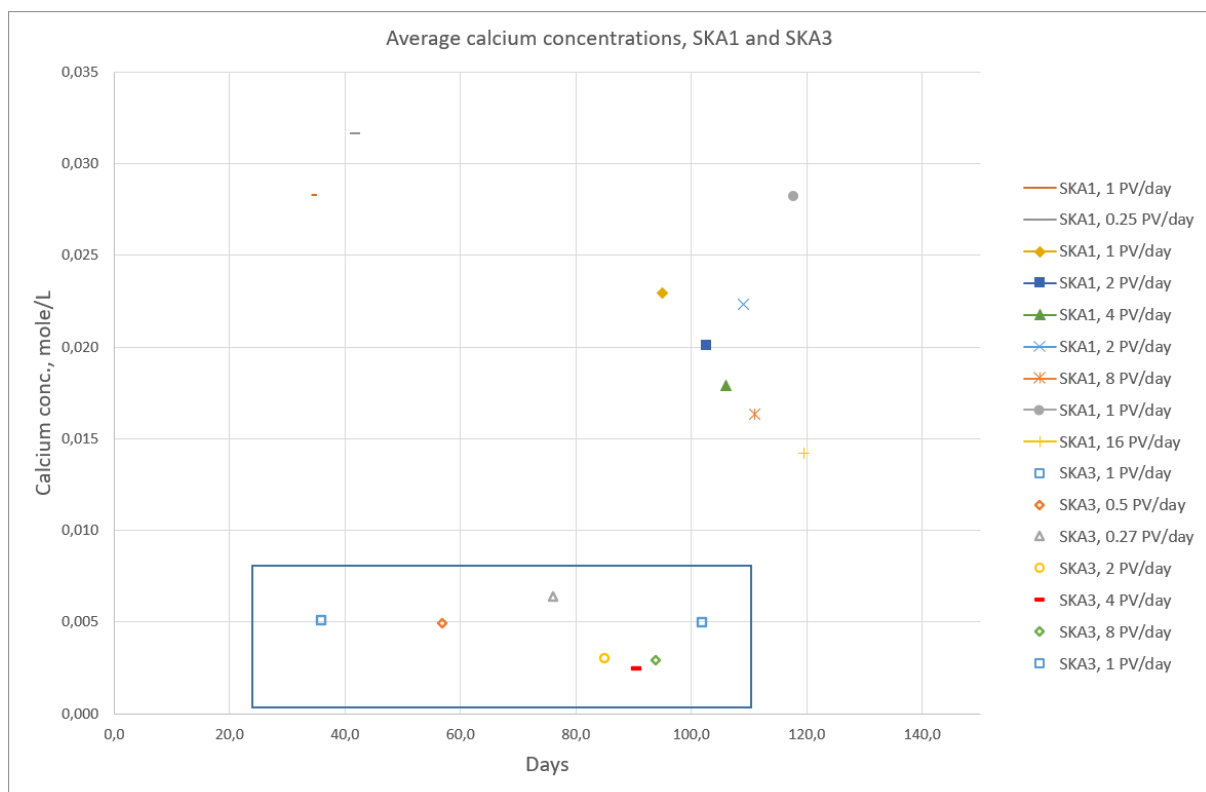

Figure 17: Measured average calcium concentrations for SKA1 and SKA3 by days. SKA3 results are found within the blue rectangle.

As we can see from these plots, temperature has a big impact on how much calcium is present in the effluents. At the lowest flowrate used during the flooding of core SKA3 less calcium was precipitated than at the highest flowrate used on core SKA1. When flooding SKA3 at 0.007 ml/min an average calcium concentration of only 0.0059 mol/L was measured, while SKA1 being flooded at 0.448 ml/min gave an average of 0.014 mol/L. At a flowrate 64 times greater

than the flowrate used on SKA3, core SKA1 still dissolved around 2.4 times as much calcium as SKA3. As stated earlier, every other parameter was the same for these tests. From the plot of SKA3 we can also see an abnormal behavior which did not occur in the flooding of SKA1. Every time the flowrate of SKA1 was lowered the concentration of calcium increased, and every time the flowrate was raised the concentration of calcium decreased. For SKA3 however, there were two instances where the concentrations behaved in the opposite way from what was expected. When lowering the rate from 0.026 ml/min to 0.013 ml/min the calcium concentration actually decreased, and when the rate was increased from 0.104 ml/min to 0.208 ml/min the concentration increased. This is likely a result of the difficulties in reaching steady state at lower temperatures, which are discussed in more detail in section 5.1.1.
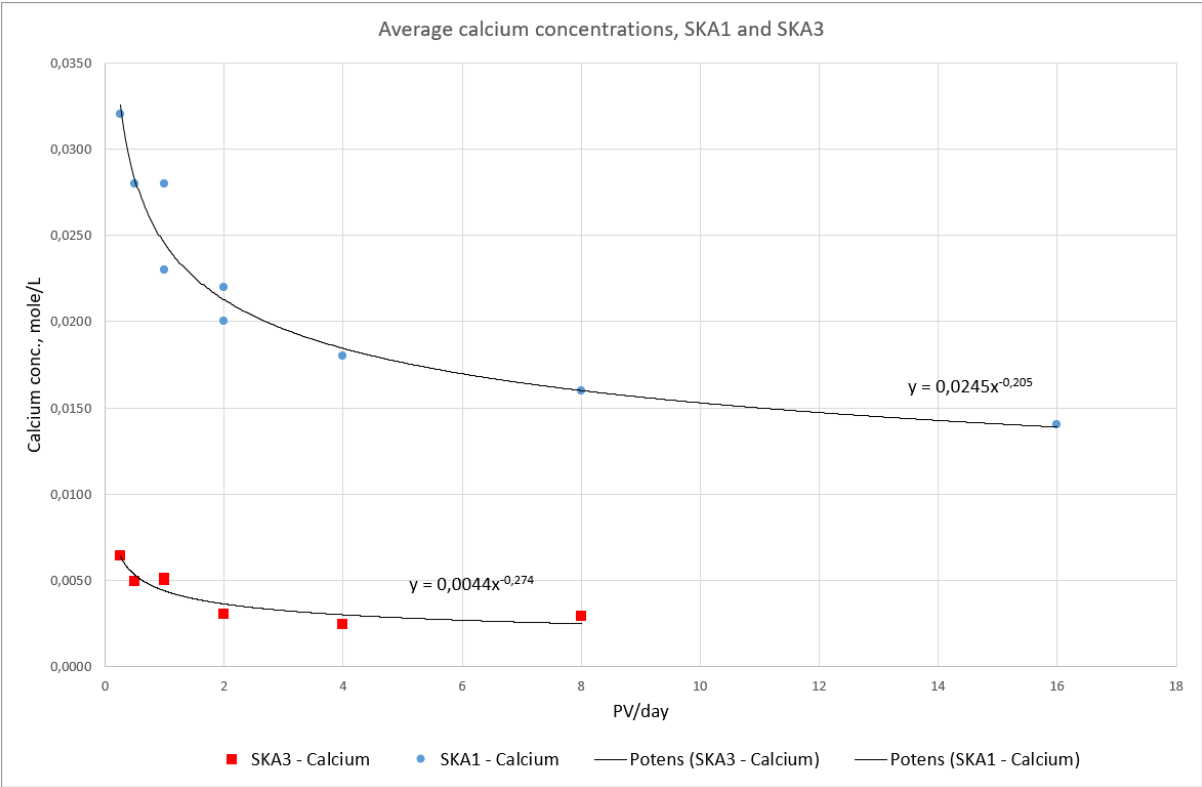

Figure 18: Measured average calcium concentrations for SKA1 and SKA3 by PV/day.

In figure 18 we have plotted the same concentrations as seen in figure 18, but this time they are plotted over PV/day instead of just over days. That SKA1 dissolves more chalk is as clear here as it is in figure 18, but now we can also see that the datapoints of both cores follow a downwards sloping pattern, with higher flowrates yielding lower concentrations. The values of SKA1 are decreasing faster than those of SKA3 at the early stages, but the rate of decrease becomes more equal through the last points.

5.2.3 Comparison with earlier tests – Chalk type

For the chalk type comparison, we will compare the average chalk calcium concentrations in the effluents of core KR30 and SKA1. Here the temperature and brine concentrations are the same, but the chalk types are different. The confining pressure is also slightly different, but we assume that this will not affect the results. The concentrations of SKA1 and KR30 will be presented in figure 19.
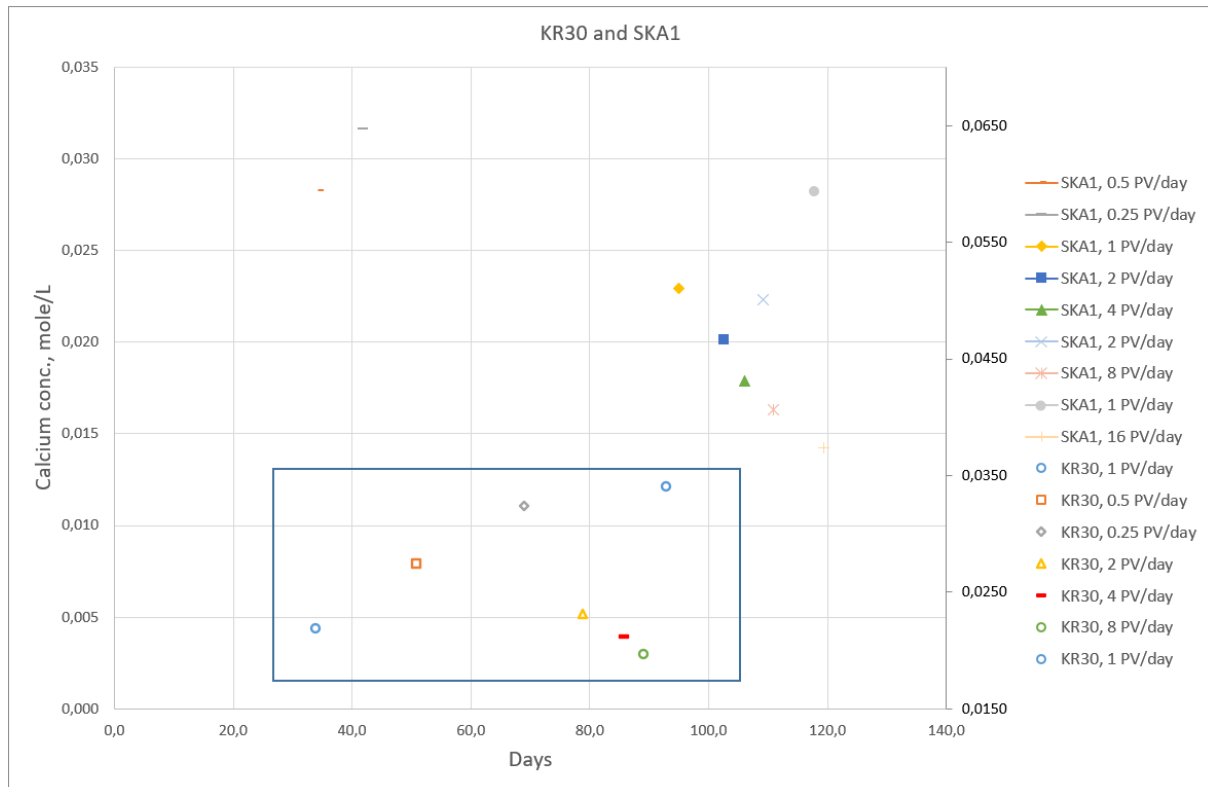

Figure 19: Average calcium concentrations for KR30 and SKA1. Results for KR30 are within the blue rectangle and its values correspond to the y-axis on the right.

In order to make the two different data sets discernible from one another I have added a secondary axis to make some air between them. Looking at the results we can see that they are much more comparable than the results for SKA3 and SKA1 were. The points with equal flowrate (in PV/day) generally yield concentrations within the same ranges. For example, KR30 flooded at 1 PV/day gave a concentration of 0.0219 mol/L at its lowest (33.9 days) and a concentration of 0.0324 mol/L at its highest (92.8 days). SKA1 also flooded at 1 PV/day yielded concentrations between 0.023 (95 days) and 0.038 mol/L (316 days). The general behavior of the concentrations for core KR30 are also more in line with the expected results. As flowrate

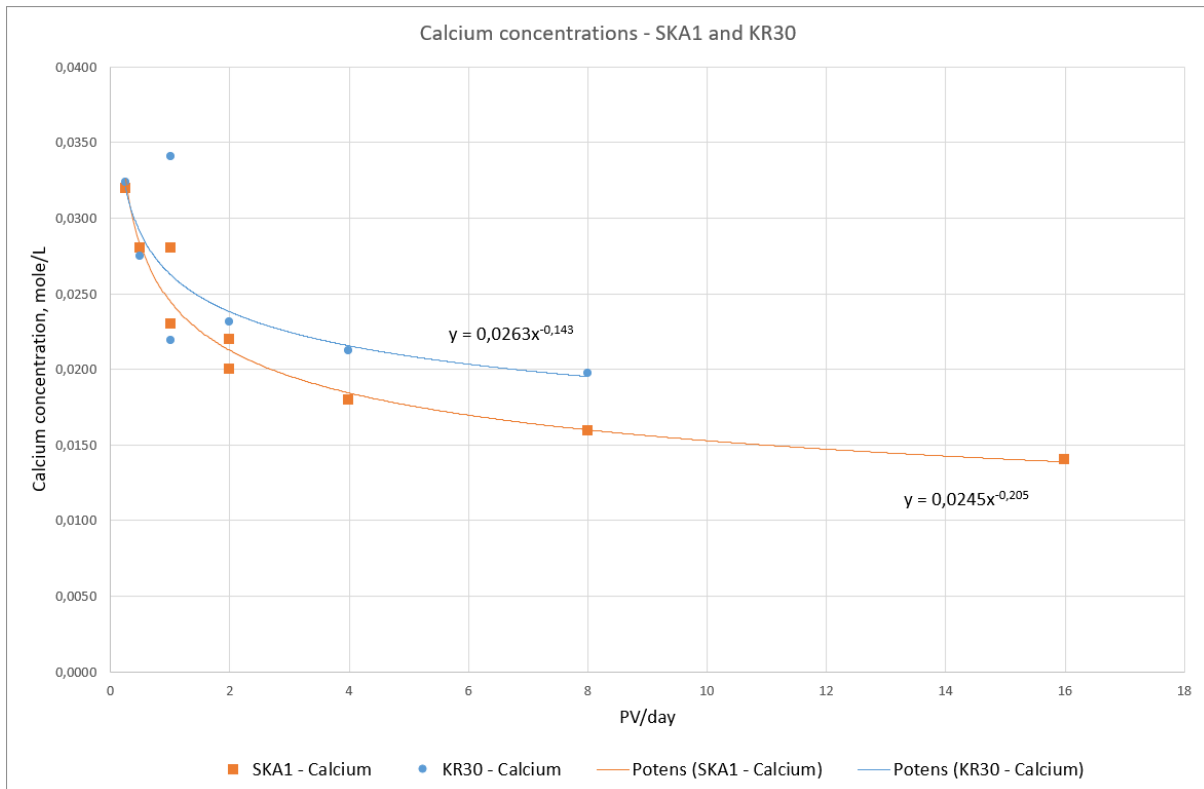decreases calcium concentration increases and vice versa.

Figure 20: Measured average calcium concentrations for SKA1 and KR30 by PV/day.

Figure 20 shows the calcium concentrations for SKA1 and KR30 by PV/day. The slopes have similar profiles to each other here, though KR30 generally dissolves more calcium than SKA1 does.

5.3   Discussion of the model

The model was designed based on the assumption that there would be a perfect substitution between magnesium and calcium. Achieving perfect substitution in practice is however quite difficult. Looking at the results we see that the measured concentrations of calcium and magnesium ions often add up to more 0.219 mol/L, the concentration of magnesium in the injected brine.

The modeled curve for SKA3 seemed to be a good fit, following the general trends exhibited by the value of the concentrations to a seemingly accurate degree. However, core SKA3 produced many erratic averages which broke our assumptions of how the concentrations should behave when the flowrate was decreased or increased. Considering that the model assumes that

a lower flowrate would mean higher concentrations of calcium every time, it is difficult to conclude with a high degree of certainty that the model is a true fit.

For core KR30 the main issue with fitting the model stemmed from the fact that the calcium concentration changed more than the magnesium concentration. When attempting to find a model which would predict both, a curve was given which seemed unideal magnesium, shown in fig. 16a and b. It is possible that either contamination in the glasses skewed the results for one of the concentrations and caused these disparaging results, but it is impossible to be certain. The results did follow the expected pattern however, which means that the assumptions made by the model was also seen in the experimental data. We therefore conclude that the tuned model for KR30 is a good fit.

These are the parameters used to tune the model for each core (Table 7).

Table 7: Values used to the models in this thesis and the thesis of (Olsen A.T., 2020)

	n	k_1	k_2
SKA3 (2021)	1.413	4.64e-08	29.05
KR30 (2021)	2.283	6.304e-08	4.858
SKA1 (2020)	1.8	8.7223e-08	6
SKA2 (2020)	1.8	3.7223e-08	1.6

We can see that most of the values are relatively close to each other in terms of their magnitude, with the k_2 value of SKA3 being an exception. As stated earlier, parameter k_2 affects the equilibrium level, n affects how fast the reaction rate based on concentration, and k_1 increases the rate. High values of k_2 and n also affect the rate. From the appendix of (Andersen et al, 2018), we see that k_2 is virtually unresponsive to concentration changes but is dependent on the temperature. A 0.219 mol/L equilibrated with calcite and magnesite gave the following results (figure 21):

Temperature (°C)	I (–)	C_{ca}^{eq} (M)	C_{mg}^{eq} (M)	$\frac{C_{ca}^{eq} + C_{mg}^{eq}}{C_{ca}^{0} + C_{mg}^{0}}$ (–)	$\frac{C_{mg}^{eq}}{C_{ca}^{eq}}$ (–)
130	0.219	0.158	0.061	1.000	0.39
110	0.219	0.148	0.072	1.000	0.49
90	0.219	0.134	0.085	1.000	0.64
60	0.219	0.106	0.113	1.000	1.07
40	0.219	0.083	0.136	1.000	1.63
25	0.219	0.065	0.154	1.000	2.35

Table A-3—0.219 M $MgCl_2$ equilibrated with calcite and magnesite at different temperatures using Phreeqc.

Figure 21: k2 values are shown in the rightmost column.

We can see that as temperature is decreased, k_2 is increased. However, in our experiments we that KR30 at 130ºC has a far lower k_2 value than SKA3 at only 100ºC. The tests done by (Olsen A.T, 2020) also has differing k_2 values, though less dramatic, despite both being run at 130ºC. The only difference between SKA1 and SKA2 was the concentration of brine being used, which should not impact the value of k_2. We would also expect k_1 to decrease with lower temperatures though this is not seen in the data either.

The same paper also found that $k_1 = 1.70 \times 10^{-8}$ for Liege chalk and 7.25×10^{-9} for Aalborg gave the best model fit for the measured concentration. These cores were also being tested at 130ºC and with a brine of 0.219 mol/L $MgCl_2$. The greatest difference is between SKA1 and Aalborg, where the k_1 value is about 12 times higher for the former than the latter. For Liege, the values are generally closer with SKA1 being 5 times higher than Liege. The values for n used by (Andersen et al, 2018) for each core were both at 2, close to the values used in this thesis and by (Olsen A.T, 2020).

6 Conclusion

The tests found that lower flowrate, meaning a longer time spent by the brine inside a core, yields an increased number of reactions between brine and core. The measured ion concentrations from the effluents of core KR30, which was flooded at 130ºC showed this exact behavior. Core SKA3 which was flooded at 100ºC gave less clear results. In this case the concentrations often had slight deviations from the expected patterns. However, it still followed a general trend of decreasing flowrate giving increased calcium concentrations.

Based on our results we have determined that temperature has a much stronger impact on the ion concentrations than the chalk type has. Our Kansas core (KR30) being flooded at 130ºC

gave far more comparable results to the core Stevns Klint core (SKA1) also being flooded at 130ºC, than our Stevns Klint core (SKA3) flooded at 100ºC did. Core SKA3 generally produced more unstable and unexpected results. This indicates that the reactions struggle to reach steady state at such low temperatures, meaning that interaction between the core and the brine is low.

The tuned model was able to predict the concentration of the effluents to a satisfactory degree for both cores, but still showed a degree of deviation from the measured concentrations. Often perfectly substitutional reactions were not achieved which skewed the model and made attaining a perfect match challenging.

7 Future work

For future experiments conducted at 100°C it would be advisable to let the experiment run for a longer period of time to ensure that the reactions at each flowrate have actually reached equilibrium. We were under time constraints to get this experiment finished within the allotted time and were therefore forced to change the flowrate when it should ideally have been left a while longer.

8 References

Andersen P.Ø., Berawala D.S., "Modeling of Creep-Compacting Outcrop Chalks Injected with Ca-Mg-Na-Cl Brines at Reservoir Conditions." *SPE J.* 24 (2019)

Andersen P.Ø., Evje S., Madland M.V., Hiorth A., A geochemical model for interpretation of chalk core flooding experiments, *Chemical Engineering Science*, Volume 84, 2012, Pages 218-241

Andersen P.Ø., Wang W., Madland M.V. *et al.* Comparative Study of Five Outcrop Chalks Flooded at Reservoir Conditions: Chemo-mechanical Behaviour and Profiles of Compositional Alteration. *Transp Porous Med* **121,** 135–181 (2018).

Appelo, C. A. J., & Postma, D. (2004). *Geochemistry, groundwater and pollution*. CRC press.

Austad T., Strand S., Høgnesen E.J., and Zhang P. "Seawater as IOR Fluid in Fractured Chalk." *Paper presented at the SPE International Symposium on Oilfield Chemistry*, The Woodlands, Texas, February 2005.

Austad T., Strand S., Madland M.V., Puntervold T., Korsnes R.I. "Seawater in Chalk: An EOR and Compaction Fluid." *Paper presented at the International Petroleum Technology Conference*, Dubai, U.A.E., December 2007.

Berg J.C. (1993). Surfactant science series volume 49, Wettability, Wetting and related phenomena

Evje S., Hiorth A., Madland, M.V., Korsnes R.I., A mathematical model relevant for weakening of chalk reservoirs due to chemical reactions. *Networks & Heterogeneous Media*, 2009, 4 (4): 755-788.

Hardman R.F.P. (1982). Chalk reservoirs of the North Sea. *Bull. geol. Soc.,* Denmark, vol. 30, pp. 119-137.

Heggheim T., Madland M.V., Risnes R., Austad T., A chemical induced enhanced weakening of chalk by seawater, *Journal of Petroleum Science and Engineering*, Volume 46, Issue 3, 2005, Pages 171-184

Hermansen H., Landa G.H., Sylte J.E., Thomas L.K., Experiences after 10 years of waterflooding the Ekofisk Field, Norway, *Journal of Petroleum Science and Engineering*, Volume 26, Issues 1–4, 2000, Pages 11-18

Korsnes R.I., Madland M.V., Austad T., Haver S., Røsland G., The effects of temperature on the water weakening of chalk by seawater, *Journal of Petroleum Science and Engineering*, Volume 60, Issues 3–4, 2008, Pages 183-193

Madland M.V., Hiorth A., Omdal E. *et al.* Chemical Alterations Induced by Rock–Fluid Interactions When Injecting Brines in High Porosity Chalks. *Transp Porous Med* **87,** 679–702 (2011).

Madland, M. V., Midgarden, K., Manafov, R., Korsnes, R. I., Kristiansen, T., & Hiorth, A. (2008, October). The effect of temperature and brine composition on the mechanical strength of Kansas chalk. In *International Symposium SCA*.

Megawati M., Hiorth A., Madland M.V. The Impact of Surface Charge on the Mechanical Behavior of High-Porosity Chalk. *Rock Mech Rock Eng* **46,** 1073–1090 (2013).

Minde, M.W. (2014). SEM image. Stavanger

Nermoen A., Korsnes R.I., Aursjø O., Madland M.V., Kjørslevik T.A.C., Østensen G. (2016). How Stress and Temperature Conditions Affect Rock-Fluid Chemistry and Mechanical Deformation. *Front. Phys*. 4:2.

Olsen A.T., Reactive flow in chalk at reservoir conditions, *un-published*, 2020

Puntervold T., Strand S., Ellouz R., Austad T., Modified seawater as a smart EOR fluid in chalk, *Journal of Petroleum Science and Engineering*, Volume 133, 2015, Pages 440-

443

Standnes D.C., Austad T., Wettability alteration in chalk: 2. Mechanism for wettability alteration from oil-wet to water-wet using surfactants, *Journal of Petroleum Science and Engineering*, Volume 28, Issue 3, 2000, Pages 123-143

Zhang P., Tweheyo M.T., Austad T., Wettability alteration and improved oil recovery by spontaneous imbibition of seawater into chalk: Impact of the potential determining ions Ca^{2+}, Mg^{2+}, and SO_4^{2-}, Colloids and Surfaces A: Physicochemical and Engineering Aspects, Volume 301, Issues 1–3, 2007, Pages 199-208